

Self-Assembly of Sodium Carboxymethyl Cellulose on Glass Surface from Evaporating Drops

Thesis Submitted by

Rohit Omar

Roll No. 211CH1262

In partial fulfillment for the award of the Degree of

Master of Technology

In

Chemical Engineering

Under the Guidance of

Dr. Santanu Paria



Department of Chemical Engineering

National Institute of Technology

Rourkela-769008, Odisha, India

May 2013



**Department of Chemical Engineering
National Institute of Technology
Rourkela – 769008, Odisha**

CERTIFICATE

This is to certify that the thesis entitled, “**Self-assembly of Sodium Carboxymethyl Cellulose on Glass Surface from Evaporating Drops**” submitted by **Rohit Omar** in partial fulfilment for their requirements for the award of Master of Technology Degree in Chemical Engineering at National Institute of Technology, Rourkela (Deemed University), is an authentic work carried out by him under my supervision and guidance.

To the best of my knowledge, the matter embodied in the thesis has not been submitted to any other University/Institute for the award of any Degree or Diploma.

Date: **24/05/2013**

Dr. Santanu Paria
Associate Professor
Department of Chemical Engineering
National Institute of Technology
Rourkela - 769008

ACKNOWLEDGEMENT

In the pursuit of this academic endeavour, I feel I have been singularly fortunate. I should fail in my duty if I do not record my profound sense of indebtedness and heartfelt gratitude to my supervisor Dr. Santanu Paria, who inspired and guided me in the pursuance of this work.

I am deeply indebted to Prof. R. K. Singh, H.O.D, Department of Chemical Engineering, National Institute of Technology, Rourkela, and all other faculties for all the facilities provided during the course of my tenure.

I want to acknowledge the support and encouragement of Mr. Naveen Noah Jason, Mr. Rajib Ghosh Chaudhuri, Mr. K. Jagajjanani Rao, Mr. Siddhartha Sankar Boxi who helped me keep a level head on my shoulders.

I thank my parents and family members for the support, encouragement and good wishes, without which I would not have been able to complete my thesis.

Rohit Omar
(211CH1262)

CONTENTS

	Title	Page No
	Certificate by Supervisor	ii
	Acknowledgement	iii
	Contents	iv-vi
	Abstract	vii
	List of Figures	viii-ix
	List of Tables	x
	Nomenclature	xi
CHAPTER 1	Introduction	1-6
	1. Introduction	2
	1.1 General Techniques for self-assembled structure fabrication	2
	1.2 Advantages of self-assembly	3
	1.3 Disadvantages of self-assembly	3
	1.4 Importance of self-assembly	3
	1.5 Applications of self-assembly	4
	1.6 Organization of thesis	6
CHAPTER 2	Background Literature	7-16
	2.1 Introduction	8
	2.2 Classification of self-assembly	8
	2.2.1 Size-discriminative self-assembly of nanospheres in Evaporating drops	9
	2.2.2 Inorganic-organic hybrid nanocrystals	11
	2.2.3 Dry Methods	13
	2.2.4 Colloidal Particles	13
	2.2.5 Polymer monolayer and nanocrystals	14
	2.3 The role of π stacking in self-assembly process	15

2.4	Concluding Remarks	16
2.5	Motivation and objective of the project	16
CHAPTER 3	Effect of Organic acid in the Self-assembled Structure of Sodium Carboxymethyl Cellulose	17-28
3.1	Introduction	18
3.2	Materials and Method	19
3.3	Results and Discussion	19
3.3.1	Effect of Acetic acid concentration with 0.1 wt.% Sodium Carboxymethyl Cellulose	19
3.3.2	Effect of Acetic acid concentration with 0.2 wt.% Sodium Carboxymethyl Cellulose	23
3.3.3	Effect of pH in the self-assembled structure of Sodium Carboxymethyl Cellulose in the presence of Acetic Acid	26
3.4	Conclusions	27
CHAPTER 4	Effect of Inorganic acid in the self-assembled structure of Sodium Carboxymethyl Cellulose	28-42
4.1	Introduction	29
4.2	Materials and Method	29
4.3	Results and Discussion	29
4.3.1	Effect of Hydrochloric acid concentration with 0.1 wt.% Sodium Carboxymethyl Cellulose	29
4.3.2	Effect of Hydrochloric acid concentration with 0.01 wt.% Sodium Carboxymethyl Cellulose	36
4.3.3	Effect of drop volume in the self-assembled structure of 0.1 wt.% Sodium Carboxymethyl Cellulose with 5 mM Hydrochloric acid	40
4.4	Conclusions	41

CHAPTER 5	Conclusions and Suggestions for Future work	42-44
5.1	Conclusions	43
5.2	Suggestions for Future work	44
	References	45-49

ABSTRACT

The advancement of modern science and technology needs day by day smaller microprocessors, chips, sensors, machines and devices, as a result the existing method of fabrication are slowly becoming obsolete. The fabrication of devices at small scale by the help of self-assembly is an inexpensive and promising technique. Evaporation of sessile droplets containing Sodium Carboxymethyl Cellulose induces outward flow within the drop, which is commonly well known as “coffee ring” effect or a dense ring like deposition along the perimeter. In this work, the formation of self-assembled structure during drying of microliter drops containing Sodium Carboxymethyl Cellulose with organic (acetic acid) as well as inorganic (hydrochloric acid) is investigated with the help of optical microscope. The structure formation is also influenced by evaporative flux and Marangoni flow inside the liquid drop. The different parameters such as sodium carboxymethyl cellulose concentration, acid concentration, drying time, drying temperature, humidity, stirring velocity, stirring temperature, pH and drop volume strongly influences the structure formation.

Keywords: Self-assembly, Sodium Carboxymethyl Cellulose, Coffee-ring effect, Sessile drop, Fractal dimension, Box-counting method.

List of Figures

Figure No.	Figure Caption	Page No.
Figure 2.1	Light microscopy image of a ring formed by slow evaporation of a drop of an aqueous suspension containing 60 nm nanospheres on mirror quality titanium disk.	9
Figure 2.2	Order-to-disorder transition in the particle stain left by an evaporating drop.	10
Figure 2.3	Nanopattern formation in self-assembled monolayers of thiol-capped Au nanocrystals.	11
Figure 2.4	The coffee ring effect structure.	14
Figure 3.1	Self-assembled structure of Sodium Carboxymethyl Cellulose with 0.1 wt.% in the presence of 5 mM Acetic acid (a, b) and 20 mM Oxalic acid (c, d).	20
Figure 3.2	$\log_{10}(\text{box size}) - \log_{10}(\text{count})$ plot for 0.1 wt.% sodium carboxymethyl cellulose with 5 mM Acetic acid (a, b) and 20 mM Oxalic acid (c, d) at different magnifications.	22
Figure 3.3	Self-assembled structure of Sodium Carboxymethyl Cellulose with 0.2 wt.% in the presence of 5 mM Acetic acid (a, b), SEM images (e, f) and 20 mM Oxalic acid (c, d).	24
Figure 3.4	$\log_{10}(\text{box size}) - \log_{10}(\text{count})$ plot for 0.2 wt.% sodium carboxymethyl cellulose with 5 mM Acetic acid (a, b) and 20 mM Oxalic acid (c, d) at different magnifications	26
Figure 3.5	Effect of pH in the self-assembled structure of Sodium Carboxymethyl cellulose (a) pH=3.5, (b) pH=4.0, (c) pH=4.5, (d) pH=5.3.	27
Figure 4.1	Self-assembled structure of Sodium Carboxymethyl Cellulose with 0.1 wt.% in the presence of 5 mM Hydrochloric acid at different magnifications.	30

Figure 4.2	Self-assembled structure of Sodium Carboxymethyl Cellulose with 0.1 wt.% in the presence of 10 mM Hydrochloric acid at different magnifications.	32
Figure 4.3	Self-assembled structure of Sodium Carboxymethyl Cellulose with 0.1 wt.% in the presence of 20 mM Hydrochloric acid at different magnifications.	33
Figure 4.4	SEM images of Self-assembled structure of Sodium Carboxymethyl Cellulose with 0.1 wt.% in the presence of 20 mM Hydrochloric acid at different magnifications.	34
Figure 4.5	Self-assembled structure of Sodium Carboxymethyl Cellulose with 0.1 wt.% in the presence of 30 mM Hydrochloric acid at different magnifications.	34
Figure 4.6	$\log_{10}(\text{box size}) - \log_{10}(\text{count})$ plot for 0.1 wt.% sodium carboxymethyl cellulose with (a) 5 mM Hydrochloric acid (b) 10 mM Hydrochloric acid (c) 20 mM Hydrochloric acid (d) 30 mM Hydrochloric acid at 400X magnification.	36
Figure 4.7	Self-assembled structures of sodium carboxymethyl cellulose (0.01 wt.%) with 5 mM Hydrochloric acid (a, b), 10 mM Hydrochloric acid (c, d), and 20 mM Hydrochloric acid (e, f); scale bars indicate 50 microns (a, c, e) and 25 microns (b, d, f).	37
Figure 4.8	$\log_{10}(\text{box size}) - \log_{10}(\text{count})$ plot for 0.01 wt.% sodium carboxymethyl cellulose with (a, b) 5 mM Hydrochloric acid, (c, d) 10 mM Hydrochloric acid, and (e, f) 20 mM Hydrochloric acid at different magnifications	39
Figure 4.9	Self-assembled structures of sodium carboxymethyl cellulose with 5 mM Hydrochloric acid (a) 1 μl , (b) 5 μl and (c) 10 μl drops and their respective magnified images (d, e, f); scale bars indicate 100 microns (a, b, c) and 25 microns (d, e, f).	41

List of Tables

Table No.	Table Caption	Page No.
Table 3.1	Fractal Analysis of images of 0.1 wt.% sodium carboxymethyl cellulose with 5 mM Acetic acid (a, b) and 20 mM Acetic acid (c, d)	22
Table 3.2	Fractal Analysis of images of 0.2 wt.% sodium carboxymethyl cellulose with 5 mM Acetic acid (a, b) and 20 mM Acetic acid (c, d)	28
Table 4.1	Fractal Analysis of images of 0.1 wt.% sodium carboxymethyl cellulose with 5 mM Hydrochloric acid	39
Table 4.2	Fractal Analysis of images of 0.1 wt.% sodium carboxymethyl cellulose with 10 mM Hydrochloric acid	40
Table 4.3	Fractal Analysis of images of 0.1 wt.% sodium carboxymethyl cellulose with 20 mM Hydrochloric acid	41
Table 4.4	Fractal Analysis of images of 0.1 wt.% sodium carboxymethyl cellulose with 30 mM Hydrochloric acid	43
Table 4.5	Fractal Analysis of images of 0.01 wt.% sodium carboxymethyl cellulose with 5 mM Hydrochloric acid (a, b), 10 mM Hydrochloric acid (c, d) and 20 mM Hydrochloric acid (e, f)	46

NOMENCLATURE

AFM	Atomic Force Microscopy
AVO	Acid Vapor Oxidation
CVD	Chemical Vapor Deposition
DLA	Diffusion Limited Aggregation
DNA	Deoxyribonucleic acid
pH	Potential of Hydrogen
pKa	Acid Dissociation Constant
SEM	Scanning Electron Microscopy
UV	Ultra Violet

Introduction

1. Introduction

Self-assembly refers to the process by which nanoparticles or other discrete components spontaneously organize due to specific interactions, through their environment. Self-assembly is typically associated with thermodynamic equilibrium, the organized structures being characterized by a minimum in the system's free energy. Essential in self-assembly is that the building blocks organize into ordered, macroscopic structures, either through direct interactions (*e.g.*, by interparticle forces), or indirectly using a template or an external field. Self-assembly is the force balance process between three classes of forces: attractive driving, repulsive opposition and directional force. Directional force can be considered functional force in the sense that it is also responsible for functionality. When only the first two classes of forces are in action, the self-assembly process is a random and usually one-step process. Self-assembly is the fundamental principle which generates structural organization on all scales from molecules to galaxies. It is defined as reversible processes in which pre-existing parts or disordered components of a pre-existing system form structures of patterns. Self-assembly typically employs asymmetric molecules that are pre-programmed to organize into well-defined supramolecular assemblies. Most common are amphiphilic surfactant molecules or polymers composed of hydrophobic and hydrophilic parts. The main driving force to self-assembled monolayers is the strong chemical bond of building units with the solid substrates and the intermolecular forces between the building units.

1.1 General Techniques for self-assembled structure fabrication

Self-assembly is basically an application of nanotechnology, therefore the method of fabrication of nanostructures is more or less same. Nevertheless it is useful to classify the methods based on the method in which synthesis occurs i.e. the dry method and solution phase method. Dry method mostly includes chemical vapor deposition, acidic vapor oxidation (Yang et al., 2009), laser ablation and so on. Solution phase method is further classified into self-assembly in bulk solution and self-assembly by partial or complete adsorption of components on a substrate. Adsorption based solution phase self-assembly mostly of fluidic and evaporation induced self-assembly methods. These methods may or may not assist by a template on a substrate. The solution phase method is most predominant gives more yield with minimal error and degree of precision is also

very high as compared to dry methods, this is proved by increasing amount of research work done in the field of electronics using self-assembly.

1.2 Advantages of self-assembly

Self-assembly has a fundamental advantage over mechanically directed assembly: It requires no machinery to move and orient components, letting random, Brownian motion do the job instead. Selective binding between uniquely matching surfaces compensates for the randomness of the motions that bring components together. Molecular synthesis methods and self-assembly can be used to produce atomically precise nanosystems by the billions, and even by the ton, thereby establishing a technology base with wide-ranging applications that can drive development forward. The architecture of biomolecular fabrication is based on the use of programmable machines to produce the complex parts necessary for self-assembly of complex systems. The same fundamental architecture can be extended to use artificial biomolecular machines (and then non-biomolecular machines), resulting in products made of better and more diverse engineering materials.

1.3 Disadvantages of self-assembly

The most fundamental disadvantage of pure self-assembly is that for every product, the structure of the parts must encode the structure of the whole. This requires that components be more complex, which tends to make design and fabrication more difficult. Another consequence is that a self-assembled product will be partitioned by complex internal interfaces that have no operational function. Unless they are strengthened after assembly, these interfaces will weak. These are major constraints. Mechanically directed assembly avoids these constraints due to components need not encode the structure of a product, they can be simple and standardized, and they can be chosen for their functional properties with less concern for how they are put together.

1.4 Importance of self-assembly

Self-assembly is scientifically interesting and technologically important for at least four reasons:

- The first is that it is centrally important in life. The cell contains an astonishing range of complex structures such as lipid membranes, folded proteins, structured nucleic acids, protein aggregates, molecular machines, and many others that form by self-assembly.

- The second is that self-assembly provides routes to a range of materials with regular structures: molecular crystals, liquid crystals, and semicrystalline and phase-separated polymers are examples.
- Third, self-assembly also occurs widely in systems of components larger than molecules, and there is great potential for its use in materials and condensed matter science.
- Fourth, self-assembly seems to offer one of the most general strategies now available for generating nanostructures.

1.5 Applications of self-assembly

Self-assembly is already an application of nanotechnology in terms of synthesis and microfabrication. Self-assembled structures are constituted of components that already have unique properties because of their small size such as in nanoparticles, their specific crystal structures or even pretreated components which assemble in a specific way such as that observed in the microelectronic part of a substrate. The basic idea of self-assembly is to bring together these different components in such a way that resultant ordered structure will have enhanced properties. The main applications of the polymer self-assembly process are as follows:

1.5.1 Polymer solar cell: Conjugate polymer based organic solar cells are considered as an important option for inexpensive renewable energy because they can be fabricated by low cost, large area printing and coating technologies on light weight flexible substrates. Bulk heterojunction (BHJ) solar cells composed of polymer: fullerene composite layer sandwiched between transparent metal-oxide anode and metallic cathode constitute one of the most successful types of polymer solar cells (Shaheen et al., 2001). The efforts on improving the performance of BHJ solar cells have been primarily focused on fundamental issues such as improved understanding of device physics, optimization of morphologies by advanced processing methods, and development of high performance materials. Polymer solar cells are light weight which is important for small autonomous sensors, potentially disposable and inexpensive to fabricate. For polymer solar cells, the nature of electrical contacts between the active organic layer and the electrodes is one of the most critical factors in determining device characteristics such as short circuit current density, open circuit voltage and the fill factor.

1.5.2 Organic Thin film Transistors: A fast switching transistor should have a high charge carrier mobility and high on/off current ratio for the semiconductor material. Self-assembly process play important role in improving device performance as well as enabling low cost processing methods for the fabrication of these devices. For organic transistors, charge injection from the electrode needs to be efficient and typically high work function electrodes such as gold, palladium and indium tin oxide are used for the p-channel organic semiconductors in which holes are generated and transported through organic material. The electrode surface modification with self-assembled monolayer is used to improve charge injection into the organic semiconductor.

1.5.3 Chemical sensing: Metal nanoparticle films are highly suitable for chemical sensing: they can be made highly porous, allowing for efficient diffusion and uptake of analyte molecules, and the conductive metal cores afford a means for signal transduction. With nanoparticle assemblies, conductance takes place through an activated electron tunneling mechanism; this leads to an extreme sensitivity to the dielectric properties of the interparticle material. Incorporation of polymer component in nanoparticle based sensor devices provides greater flexibility than simple nanoparticle assemblies. First, the utilization of flexible polymers to space nanoparticles increases the interparticle space and film porosity. Second, the polymer provides multiple interaction sites that can be designed to allow for specific interaction with analyte molecules. Third, the polymer can be designed to enable crosslinking of the nanoparticles, resulting in a mechanically reinforced film. Taken together, these virtues of nanoparticle – polymer composites all contribute to enhanced selectivity and sensitivity.

1.5.4 Catalysis: Noble metals such as palladium and platinum are used for catalysis in numerous important chemical transformations. To achieve a high performance to cost ratio, catalysts are required to have, amongst other important attributes, a large surface area of catalytically active metal. Nanoparticles are highly suitable to serve as catalysis. Moreover, catalysis with these systems often occurs at vertices and defects, which are much more prevalent in nanoparticle systems. Use of polymers for catalyst design has originated from the ability to easily separate the resin based catalyst from the reaction mixture. Metal nanoparticles combined with polymers are utilized to serve as matrices with confined cavities. A general drawback of catalysts made of

nanoparticle-polymer composites is that the polymer encasing the nanoparticles hinders diffusion of substrates and products to and from the catalytic centers. This results in reduced efficiency (in terms of mass transport of both reactants and products) of these catalysts, despite the relatively high surface area afforded by nanoparticles. Rotello and co-workers have employed the polymer mediated nanoparticle networks as precursor for catalyst fabrication.

1.6 Organization of Thesis

The thesis has been divided into five chapters. Chapter-1 is an introduction to self-assembly. Here, a brief history of self-assembly is given followed by the general definition of self-assembly. Then the focus is on the different techniques including advantages, disadvantages, importance and applications of self-assembly. Chapter-2 is an exhaustive literature review on self-assembly techniques such as dry methods and wet methods, the different materials used to fabricate self-assembled structures along with the applications. Chapter-3 deals with the effect of organic acid in the self-assembled structure of sodium carboxymethyl cellulose. Chapter-4 deals with the effect of inorganic acid in the self-assembled structure of sodium carboxymethyl cellulose. Chapter-5 concludes the research work described here and also contains few suggestions for future work.

Background Literature

2.1 Introduction

Self-assembly formation of nano or colloidal particles can be broadly classified into “dry methods” (Dick et al., 2004; Cheng et al., 2009) and “liquid phase methods” (Burda et al., 2005; Qi.,2010). Formation in dry condition include chemical vapor deposition, laser ablation etc. Liquid phase formation of self- assembly can again be classified into (1) inside the bulk media and (2) onto the solid surface. Self-assembly onto the solid surface may occur because of the adsorption of the particles on the surface (Bai et al., 2008; Banerjee et al., 2009) or during the evaporation of a liquid drop (Denkov et al., 1992; Deegan et al., 1997).

Until recently most aggressive procedures such as extreme lithographic techniques using extremed UV, focused ion beam, electron beam etc. have been used to create nanostructures on metal and polymer substrates. Other processes such as CVD, laser ablation, where the nanostructures are formed as by-products during manufacture of functionalized or seeded carbon nanotube obviously have no scope for scale up or mass manufacture processes. Hence there exists a need for a method that will enable fabrication of nanostructures in a simple and efficient manner with minimal wastage of precursors. The self-assembly as a nanostructure process is so attractive due to it generates the building units which in turn self-assemble into complex structure in order to attain to a low energy state.

2.2 Classification of Self-assembly

Self-assembly can be broadly classified into two domains based on the media on which the whole process occurs, these two domains being liquid phase methods and the dry methods. The solution phase method being so diverse is again subdivided according to the components involved in the self-assembled structures such as particles, nanocrystals and micro-machined parts. Here the term particles is strictly in reference to nanoparticles such as latex, glass spheres, polymer and other type of particles which have been formed as a result of precipitation reaction and bear somewhat more attraction towards each other than towards the solvent. Although nanocrystals are also formed as a result of precipitation reaction.

Self-assembly can also be classified as either static or dynamic self-assembly. Static self-assembly involves systems that are at global or local equilibrium and do not dissipate energy. For example, molecular crystals are formed by static self-assembly; so are most folded, globular proteins. In static self-assembly, formation of the ordered structure may require energy (for

example in the form of stirring), but once it is formed, it is stable. In dynamic self-assembly, the interactions responsible for the formation of structures or patterns between components only occur if the system is dissipating energy. The patterns formed by competition between reaction and diffusion in oscillating chemical reactions are simple examples; biological cells are much more complex ones. In templated self-assembly, interactions between the components and regular features in their environment determine the structures that form. A broad range of objects such as carbon nanotubes, block-copolymers, viruses or DNA molecules can be used as templates for nanoparticle organization. Strong interactions between a template and nanoparticles lead to the arrangement of nanoparticles in structures that are predefined by the shape of the template.

2.2.1 Size-discriminative self-assembly of nanospheres in evaporating drops

Evaporation of liquid drops containing nanospheres resulted in circular deposition patterns. The circularity of the patterns depended on the uniformity of the surface tension on the substrate. By employing binary suspensions, containing two differently sized nanospheres, it was possible to modulate the fine structure of such rings. Slow evaporation on mirror-polished substrates resulted in well-ordered distributions, where larger particles self-assembled in dense hexagonal packages, forming apparently an external ring, deposited around the massive inner ring. Deposition started at the air/liquid/solid-contact line. Results could inspire principles for the fabrication of optical devices and may be fruitfully used to design biomaterials with cell-selective properties (Sommer et al., 2004).

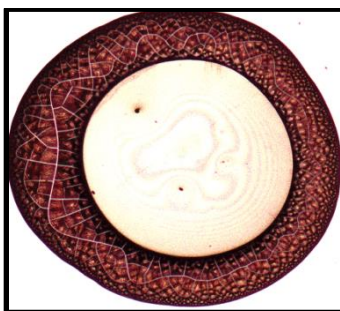


Figure 2.1 Light microscopy image of a ring formed by slow evaporation of a drop of an aqueous suspension containing 60 nm nanospheres on mirror quality titanium disk (Sommer et al., 2004).

A simple model is employed to predict the radial arrangement of nanospheres in rings. Deviations from a standard order (predicted by the model) may be useful to detect biologically active nanoparticles. Ring formation has been described for various nanoparticles: silver, copper, cobalt, cadmium sulfide, barium ferrite, and gold. The mechanism of formation has been explained in terms of the interaction between wetting properties, capillary forces, surface tension, and evaporation-driven convective flows resulting from temperature gradient. However, for nanoparticles suspended in liquid drops, gravity is likely to considerably affect both dynamics (rate of sedimentation) and pattern formation in the rings. Ordered arrays of colloidal particles present important characteristics for fields as photonics and biotechnology. A relatively simple approach to deposit particles onto a substrate is by evaporation of a colloidal dispersion droplet. In droplets with pinned contact lines, evaporation gives rise to the so-called coffee-stain effect (Marin et al., 2011). In an evaporating drop with an immobile contact line, a capillary flow is generated to replenish the liquid that has evaporated from the edges. This flow drags particles towards the contact line, forming the ring-shaped stain in particle suspensions such as coffee (Deegan et al., 1997).

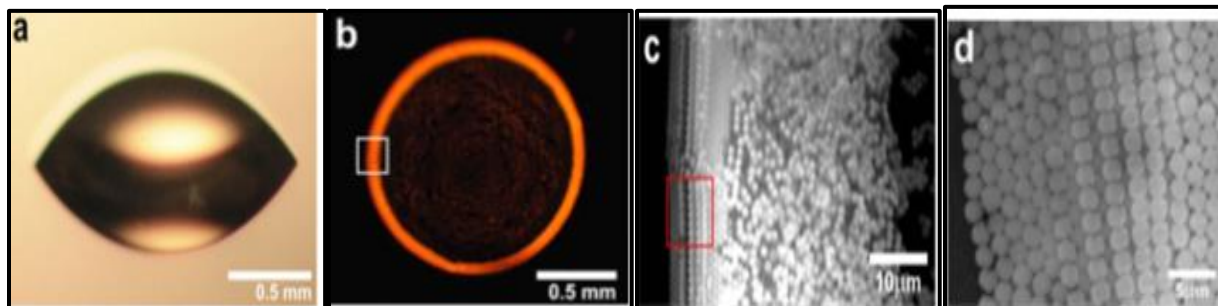


Figure 2.2 Order-to-disorder transition in the particle stain left by an evaporating drop.

When the droplet has completely evaporated, most of the colloidal particles have aggregated into a ring-shaped coffee stain Fig. 2.2(b). Zooming in on the stain, we see that the particle arrangement is not homogeneous as shown in Fig. 2.2(c); there is a remarkable transition from a crystalline arrangement to a disordered phase. A top view of the stain, Fig. 2.2(d) shows a sequence of particle arrangements within the ordered phase, starting from hexagonal packing, followed by square packing, and again hexagonal packing.

2.2.2 Inorganic-organic hybrid nanocrystals

The recent work by Banerjee et al. highlights a drying mediated process to form self-assembled monolayers of thiol-capped gold nanocrystals. They have used dodecane capped gold particles suspended in toluene, which is then spread on a Langmuir trough. The thiol capped gold particles being hydrophobic float on the water surface and after the solvent evaporates, a monolayer of particles is formed at the air-water interface. Using the Langmuir troughs, the surface-pressure isotherms were studied for the films transferred at 2, 5, 10, 12 and 14 mN/m. The isotherms reveal distinct gaseous, liquid-expanded and liquid-condensed phases but more than they reveal that with the increase in compression more pattern formation is observed. They explained that pattern formation is triggered by the spreading process in Langmuir trough itself. Due to spreading, some of the particles adventently coalesce, given the tendency to kinetically self-assemble and once the monolayer formed by these particles is transferred onto the substrate (carbon coated grid), these groups of particles are further brought together due to the drying process and the interface of forces.

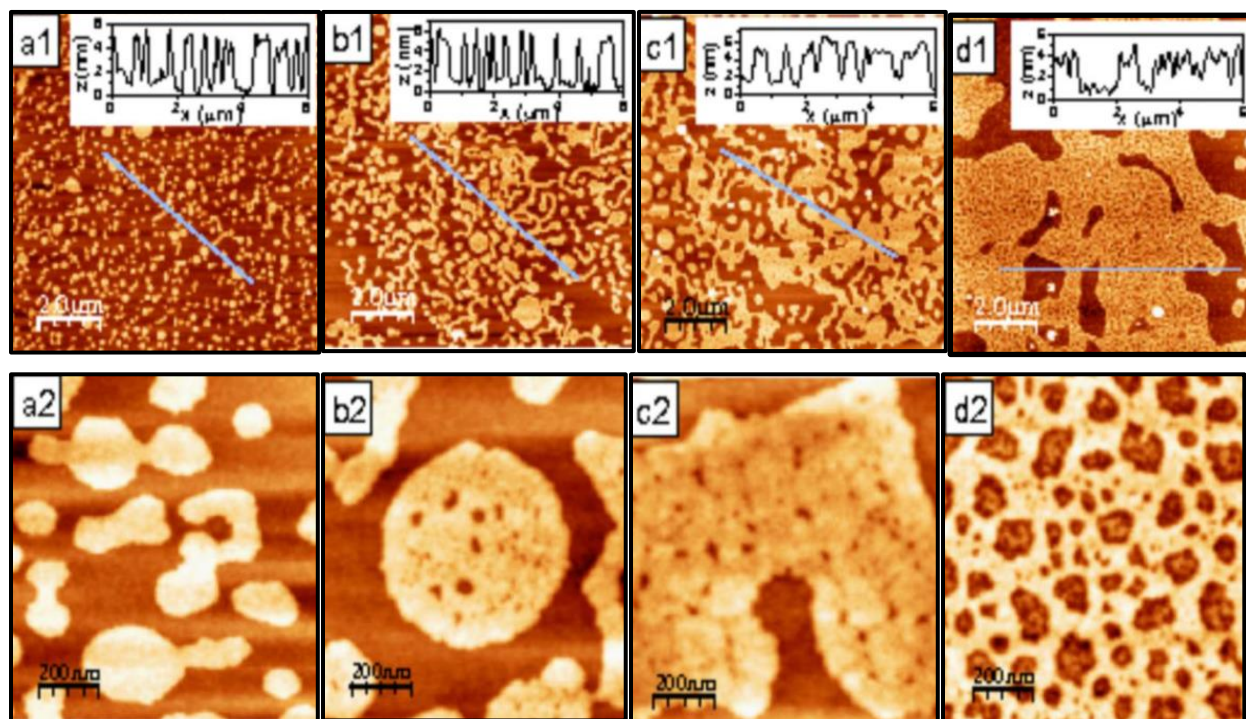


Figure 2.3 Nanopattern formation in self-assembled monolayers of thiol-capped Au nanocrystals (Banerjee et al., 2009).

During the drying process, the water trapped in these groups of particles first start as nucleation centers within these particle agglomerates and later grows into bigger water bodies by combining with other such isolated bodies of water. Then later due to compression they begin to force their way out of particle agglomerates and while moving the advancing water front carries with it any loose nanoparticles and until just before total dry-out the particles are deposited on the pathways of water fronts. This is attributed to be one of the initial reasons for the pattern formation. Later the water from the various particle islands are suspected. Apart from the said reason drying mediated self-assembly is always accompanied by contrarotatory hydrodynamic convection (Bernard-Marangoni convection) and the kind of pattern that is formed also suggests spinodal decomposition and dewetting.

Another very similar work by John et al. (John et al., 2010) also using dodecanethiol capped gold nanoparticles suspended in toluene, describe the formation of cellular networks but they have limited their scope to SEM and AFM studies. They describe how by capping nanoparticles with molecules and ligands with a tendency to self-assembly, the nanoparticles acquire an ability to self-assemble themselves. Molecules such as alkanethiols, alkyl amines and biomolecules allow programmed self-assembly to be achieved. They use mica as their substrate instead the silicon substrate with its native oxide described in the work by Banerjee et al. (Banerjee et al., 2009). Through their AFM studies they able to explain why water appears as nucleation and growth centers in the middle of the chunks of agglomerated particles; something which was unclear in the previous. In the field emission SEM studies operating at low vacuum, water vapor was gradually introduced in the chamber. This causes water to get adsorbed on the hydrophilic mica surface and form monolayers and most importantly microdomains, which act as nucleation and growth sites for water holes and as described in this study, they grow to form water domains. The hydrophobic thiol capped gold particles which are weakly adhered to the mica surface are able to move and diffuse better. It has also been noted in many colloidal nanocrystal synthesis procedures that the surfactants which usually play the role of restricting further growth by surface adsorption, also play a key for connectivity and self-assembly to occur among the nanocrystals. Although there are many ways to synthesize colloidal nanocrystals but the methods for size, shape control and establishing connectivity between monomers are fundamentally the same. A wide range of nanocrystals including metals, metal oxides, sulfides and many semiconductor materials are synthesized recently.

2.2.3 Dry Methods

Dry methods and strategies for synthesizing nanostructures are limited and not very diverse. They mostly consist of Chemical vapor deposition technique, laser ablation and variation of these two techniques based upon the precursors used. Most nanostructures are synthesized using materials with semiconductor properties, so that they can have application as transparent conductive films, transparent field effect transistors, optical devices, sensors, solar cells and photocatalysis. Metal oxides such as ZnO, MgO, SnO₂, ZnS have been studied extensively in this area (Lao et al., 2002; Ma et al., 2003). Lao et al. have managed to generate large no. of unique nanostructures using ZnO using their unique CVD method. In their process they insert the required oxides and graphite powder into sealed end of a small quartz tube. Then the substrate is placed at the open end of the tube, after which the open end is covered by graphite foil. The whole arrangement is then placed inside the ceramic tube of a tube furnace at 0.5-2.5 torr and at 950-1050°C for 15-30 minutes. After cooling of the whole arrangements, the nanostructures were deposited on the substrate and on the graphite foil. Using this method, they were able to synthesize nanonails on nanowires/nanobelts, ZnO nanorods on nanobelts and other hierarchical ZnO structures.

2.2.4 Colloidal Particles

The fabrication of self-assembled nanostructure approach is very simplest, energy efficient and economically viable compared to all other methods. These methods are often one-pot process requiring no special conditions or expensive instruments to be carried out. The self-assembly of colloidal particles can be carried out using virtually any particle ranging from SiO₂ particles, polymer particles, glass particles or even particles synthesized in the reaction media where the particle solution is directly used for self-assembly purposes and on any substrate for that matter. (Bharadwaj et al., 2009, 2010). The structure formed at the edge of drop is depends heavily on the interaction between the particle, the substrate and the carrier fluid of the particles. The work which pioneered the whole race of self-assembly using colloidal particles was by Deegan et al., 1997. In their experiments ring like patterns formed from dried liquid drops, now famously called “coffee ring” effect.

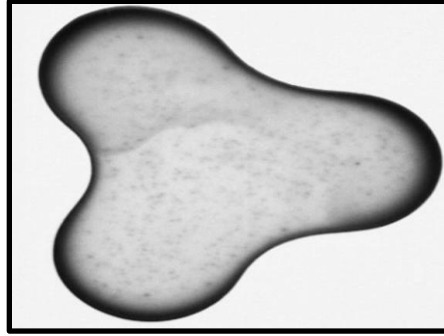


Figure 2.4The coffee ring effect structure (Deegan et al., 1997).

They state that capillary force in the drop are responsible for holding the particles together at the boundary of the drop, where the effect of force is maximum because of liquid height, which is very low there, allowing for the capillary force to actually function by forming menisci around the particles and also due to large no. of particles there. The presence of any kind of salt or solute is said to in the formation of flow called the marangoni flow, which very often flows in the opposite direction of the flow of liquid to replenish the fluid lost in evaporation from boundary. Kralchevsky and Nagayama have contributed much to this field in terms of understanding the capillary forces between different type of particles, phenomenon like size dependent segregation of particles, formation of organized two dimensional arrays of particles etc.

Recent studies shows that the factors related to the self-assembly process are very complex. The study by Vancea et al. determines different conditions under which particles form patterns. Their study indicates that variation in particle concentration and particle mobility are key factors deciding the final structure. The presence of instabilities causing the “fingering” patterns which is actually beginning the formation of branch and leaf like patterns by the self-assembled particles, may also be responsible. This is indicative of instabilities like Mullins Sekerka instability which may occur due to presence of salts in the particle solution and salts also contributes to marangoni flows.

2.2.5 Polymer monolayer and nanocrystals

Semicrystalline polymers have been used to prepare self-assembled monolayers at air-water interface and these monolayers have been extensively studied. Most of the studies have been focused on self-organization of polymer chains at the growth front in regard to the kinetic pathway followed by the polymer melt. It has been observed that monolayers, which are hugely

consisted of polymer nanocrystals also often exhibit crystal morphologies such as dendrites, spherulites and other branched fractal structures, where the fractal and branched morphologies are limited to thin films while the spherulitic and single crystal growth are observed most on case of bulk films. In case of polyethylene oxide, the thickness of thin films is in the vicinity of around 10 nm. Preparation of thin monolayers of these polymers often involves spreading the polymer solution into thin films, often in a Langmuir trough as it is possible to make in situ observations of the whole growth process and the different morphological parameters such as branching angle, thickness, the growth of dendritic fingers; or the other method is to spin cast the polymer solution or melt onto a substrate. It is well known that decreasing film thickness has a dramatic effect on molecular mobility, glass transition temperature and segmental orientation of semicrystalline polymers. It has been previously reported that the main cause of different crystal morphologies is diffusion-limited crystal growth.

2.3 The role of π stacking in self-assembly process

Interactions between aromatic units play a central role in many areas of chemistry and biochemistry, most notably in molecular recognition and self-assembly. Aromatic rings tend to form high-order clusters of four different types: parallel displaced, T- shaped, parallel staggered, or Herringbone. All four geometries are possible potential minimum configurations in the Lennard-Jones-Coulomb empirical potential calculations. The attractive nonbonded interactions between planar aromatic rings are referred to as π - π interactions or π -stacking (Gazit E., 2002). The steric constrains associated with the formation of these ordered stacking structures have a fundamental role in self-assembly processes leading to the formation of supramolecular structures. Such π stacking interactions stabilize the double-helix structure of DNA involved in core packing and stabilization of the tertiary structure of proteins, host– guest interactions, and porphyrin aggregation in solution. In macroscopic devices, Self-assembly based on selective control of non-covalent interactions provides a powerful tool for the creation of structured systems at a molecular level, and application of this methodology to macromolecular systems provides a means for extending such structures to macroscopic length scale. Monolayer - functionalized nanoparticles can be made with a wide variety of metallic and nonmetallic cores, providing a versatile building block for such approaches (Boal et al., 2000).

2.4 Concluding Remarks

The self-assembly process have been classified into many sections above. Of these it is easily understandable that the solution processes are far more efficient and have a higher throughput and also have higher chances of being scaled up into a fully-fledged industrial process. The dry methods although very novel and produce attractive materials, they are simply not very feasible for very large scale production. In the solution phase methods, for template assisted and non-template assisted methods each have their own advantages. Template assisted methods require the components and substrate to be pretreated, but these methods have immediate applications in the field of electronics and optics. On the other hand, non-template assisted methods require no pretreatment of any kind but they still lack the accuracy required for applications in electronics. However, these methods have immediate applications such as wetting, printing and other adsorption based applications. On the whole they are very attractive and novel applications for nanostructure fabricated self-assembly. The whole top-down approach might slowly be phased out in favor of self-assembly methods and with the inherent advantage of being a green method; this seems a very logical choice.

2.5 Motivation and objective of the project

Among many different methods that are available for the fabrication of structures and surface modification on the micro-nano scale, self-assembly stands out to be simplest, most efficient and highest yielding method. The formation of polymeric self-assembled structures is useful in various applications such as polymer solar cell, organic thin film transistors, chemical sensing, and catalysis etc. In this work, the formation of self-assembled fractal “tree” like patterns are observed using pure Sodium Carboxymethyl Cellulose (weak anionic polyelectrolyte) with oxalic acid as well as hydrochloric acid. The primary objectives of the project are as follows:

- (i) To explore the mechanism of self-assembled structure using Sodium Carboxymethyl Cellulose on flat surface after evaporating sessile drops.
- (ii) To study different parameters such as cellulose concentration, acid concentration, basicity of acids, pH, and drop size on affecting the self-assembled patterns.

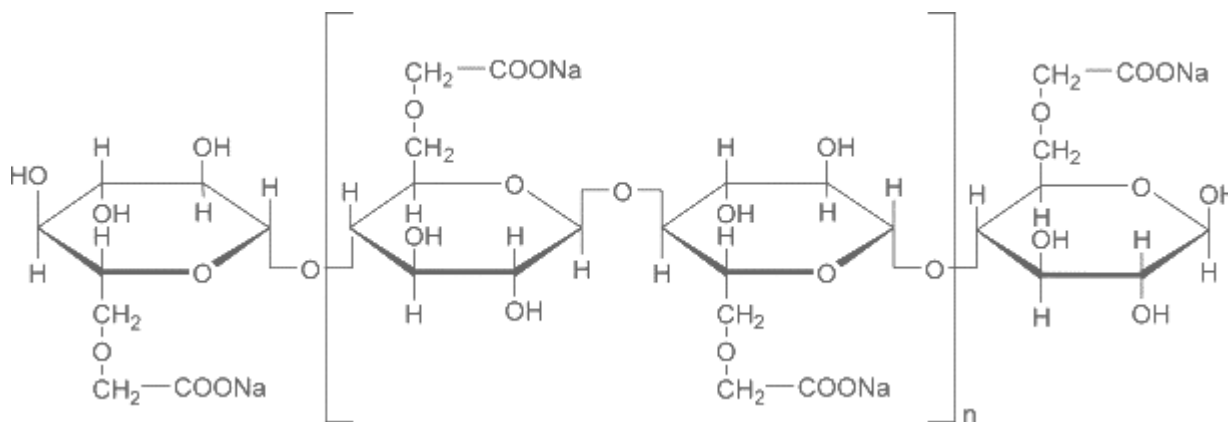
Effect of Organic acid in the self-assembled structure of Sodium Carboxymethyl Cellulose

3.1 Introduction

Nanostructured surfaces are prepared primarily by two techniques: Lithography and self-assembly. Out of these two techniques, self-assembly is simple and less cost effective. Self-assembly result from evolution of a system based on kinetic and thermodynamic considerations. The formation of self-assembled structure results due to crystal growth. In crystal growth, periodic arrangement of atoms results from the energy and entropy considerations. Another interested example of self-assembly is thin film growth. In thin film growth from the vapor phase, atoms are adsorbed on the surface, subsequent adatom diffusion and relevant interaction to the substrate.

The term polyelectrolyte is meant a high molecular weight substance that is simultaneously also an electrolyte containing a number of ionizable groups distributed along the polymer chain. Carboxymethyl cellulose is a cellulose derivative with carboxymethyl groups ($-\text{CH}_2\text{-COOH}$) bound to some of the hydroxyl groups of the glucopyranose monomers that make up the cellulose backbone. In other words, it is a compound of cellulose in which some of the cellulose $-\text{OH}$ groups have been converted into a structure of the type $-\text{O-CH}_2\text{-COOH}$. The polyelectrolytes dissociate into a macroion and counterions in aqueous solution.

Structure of Sodium Carboxymethyl Cellulose



One typical feature of the polyelectrolytes is the extremely low activity coefficient of the counterion. If the charge density of polyelectrolyte is high enough, a fraction of counterions is located in the vicinity or at the surface of macroion (condensed fraction of counterions). The physical background of the counterion-condensation effect is the competition between a gain in

energy in the electrostatic interaction and a loss of entropy in the free energy. Another interesting feature of the polyelectrolytes is the high expansion or ‘stretching’ of the polyion chain due to strong electrostatic repulsion between charged segments (Gennes P-G, D., 1976).

3.2 Materials and Method

The chemicals used in this experiment were procured from the following companies, Sodium Carboxymethyl Cellulose $[C_6H_7O_2(OH)_x(OCH_2COONa)_y]_n$ 99% purity from Loba chemicals (India), Acetic acid (CH_3COOH) 100% purity from Merck (India). All chemicals were used as received without any further purification. Ultrapure water having resistivity of 18 M Ω cm and pH 6.4–6.5 was used for all the experiments.

Sodium Carboxymethyl Cellulose in aqueous media was prepared from the stock solution of higher concentration with acid. The proper mixing of cellulose and acid proceeded by magnetic stirrer with continuous stirring at 600 rpm maintaining the temperature at 30°C about 20 minutes. The glass slides were initially washed with alcohol and then deionized water, and dried in a hot air oven. Then the solution was dropped onto the glass slide using a microliter syringe (Hamilton) with different drop volumes (1 μ l to 10 μ l) to study the drop volume also. Then the slides containing droplets were dried in a hot air oven at 30°C for more than 210 minutes with a constant relative humidity of 30%. The resulting dried drops were observed under an optical microscope (Hund, D600).

3.3 Results and Discussion

3.3.1 Effect of Acetic acid concentration with 0.1 wt.% Sodium Carboxymethyl Cellulose

Self-assembled structures of cellulose on hydrophilic glass surface after drying of small drops were studied using an optical microscope. The structures presented here are definitely an example of dendritic crystallization because of the presence of the crystallizable sodium acetate salt and the cellulose molecules. Hence the structures formed here also follow a natural fractal pattern, but under the influence of the coffee-ring effect and Marangoni flows. The Marangoni effect gives way to Mullins-Sekerka instability which causes stems of the structure to grow along the perimeter towards the center. This lends uniqueness to the fractal patterns, apart from the basic structure the branches would follow depending on the unit cell of the salt crystal. Now in the present study, it is evident that the structures tend to grow from the perimeter towards the

center of the drop and the structures seem too organized and well formed to be simply attributed to diffusion limited aggregation (DLA).

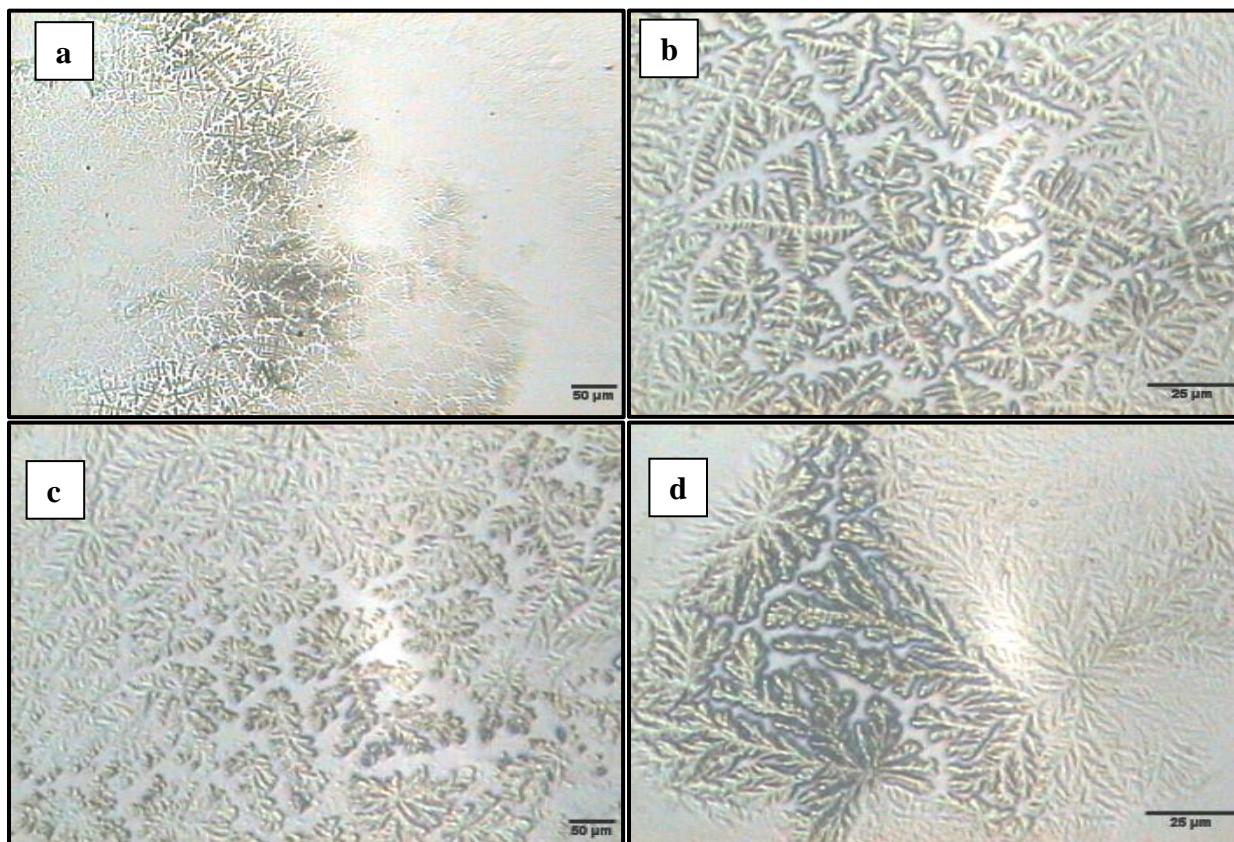


Figure 3.1 Self-assembled structure of Sodium Carboxymethyl Cellulose with 0.1 wt.% in the presence of 5 mM Acetic acid (a, b) and 20 mM Acetic acid (c, d).

The formation of fractal tree like pattern at the periphery of the drop is to be supported by fractal dimension, which is analyzed by Fractal Analysis Software (Sasaki et al., 1994). Fractal dimension is the main tool used to describe the fractal geometry and the heterogeneity of irregular shapes. It allows capturing what is lost in traditional geometrical representations of shapes. For a fractal curve that lies completely within two dimensional plane, the fractal dimension is greater than one (the Euclidean dimension of curve). The closer fractal dimension is to one, the smoother the fractal curve. If fractal dimension becomes two, we have Peano curve that is the curve completely fills a finite region of two dimensional spaces. The fractal dimensions of these two curves at lower and higher magnification are 1.8084 and 1.8178 respectively with correlation coefficient of 0.99. On the other hand, fractal dimension of the

curves at higher acid concentration with 0.1 wt.% sodium carboxymethyl cellulose increases which corresponds to 1.7708 and 1.8143 as well as coverage percentage or difference of brightness increases. This fractal dimension value gives a quantitative measure of the self-similarity of the structures and their increasing complexity with length scale. This demonstrates that higher acid concentration with constant cellulose concentration the structure becomes less fractal as well as dense. It should be noted that there is a linear relationship between coverage percentage and fractal dimension and if lower the fractal dimension, it attains smoothness. The table 3.1 also depicts that item of coverage changes the difference of brightness depending on the image. Fractal dimension of cellulose fractal “trees” and their shapes likely indicate that these fractal “trees” are formed via diffusion limited aggregation (DLA) process.

Table 3.1: Fractal Analysis of images of 0.1 wt.% sodium carboxymethylcellulose with 5 mM Acetic acid (a, b) and 20 mM Acetic acid (c, d)

Image no.	Width, height	Coverage (%)	Correlation coefficient	No. of data to calculate	Fractal Dimension
a	640, 480	30.4	0.9972	8	1.7708
b	640, 480	38.6	0.9982	8	1.8143
c	640, 480	35.0	0.9979	8	1.7950
d	640, 480	32.6	0.9978	8	1.7753

The graph between $\log_{10}(\text{box size}) - \log_{10}(\text{count})$ are also displayed whether to check the image is fractal or not by linearity with Fractal Analysis Software (Sasaki et al., 1994). The box-counting method provides the grids with a varying number of boxes are superimposed on an image of the pattern of interest. If a structure is fractal (i.e., self-similar over multiple scales of dimension), the log of the number of boxes that are filled plotted against the log of the total number of boxes yields a straight line. It is proposed to assign the smallest number of boxes to cover the entire image surface at each selected scale as required, thereby yielding more accurate estimates. Fractal pattern introduces spaces of a range of sizes. So that there is hierarchy of space sizes including few large and many small spaces. On the other hand if the spaces are all about the same size with tightly packed, there is no hierarchy of structure that characterizes fractals. The inset of box counting is to quantify fractal scaling but from a practical perspective this would require the scaling be known. In fractal analysis, however, the scaling factor is not always known ahead of time, so box counting algorithms attempt to find an optimized way of cutting a pattern

up that will reveal the scaling factor. The fundamental method for doing this starts with a set of measuring elements – boxes - consisting of an arbitrary number, called E for convenience of sizes, which we will call the set of ϵ s. Then these ϵ -sized boxes are applied to the pattern and counted. To do this, for each ϵ in E, a measuring element that is typically a 2-dimensional square or 3-dimensional box with side length corresponding to ϵ is used to scan a pattern or data set (e.g., an image or object) according to a predetermined scanning plan to cover the relevant part of the data set, recording, i.e., counting, for each step in the scan relevant features captured within the measuring element.

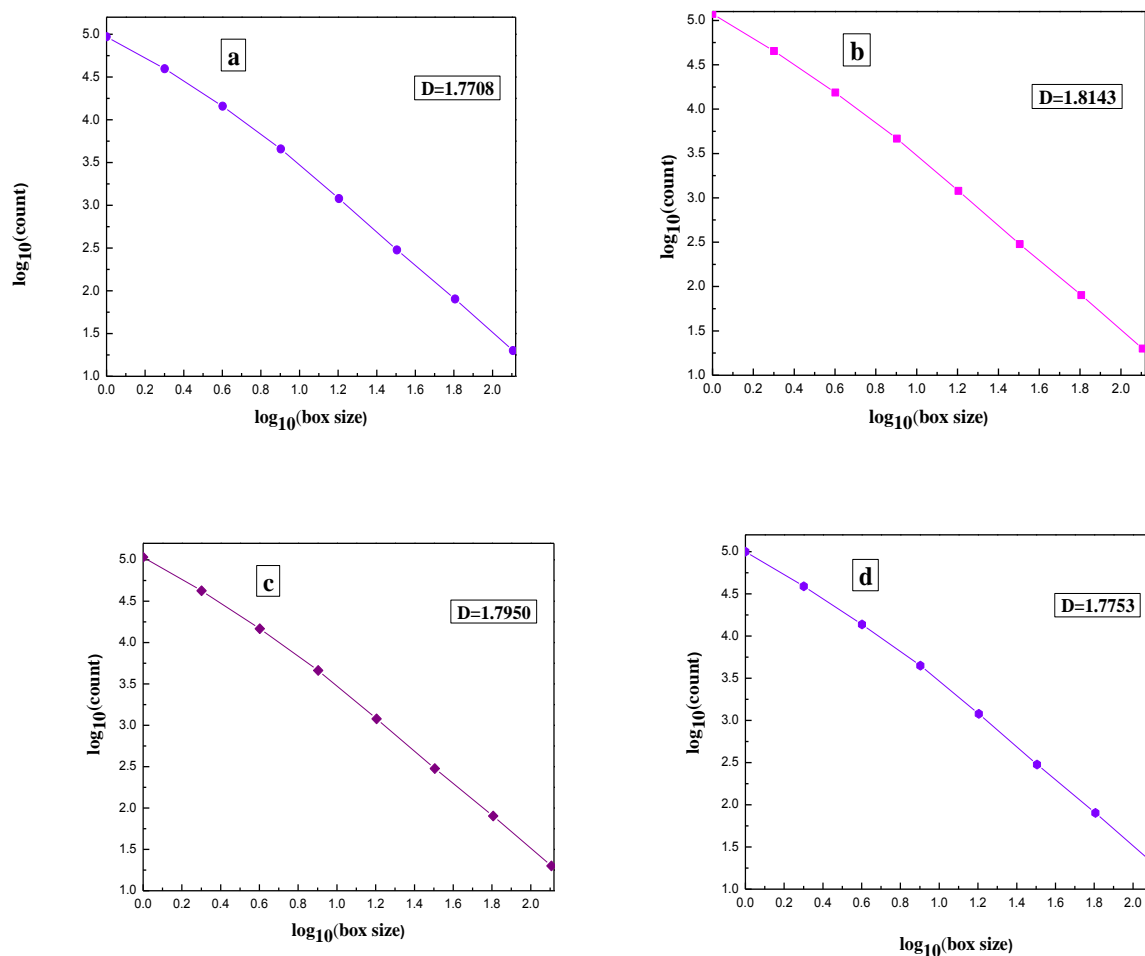
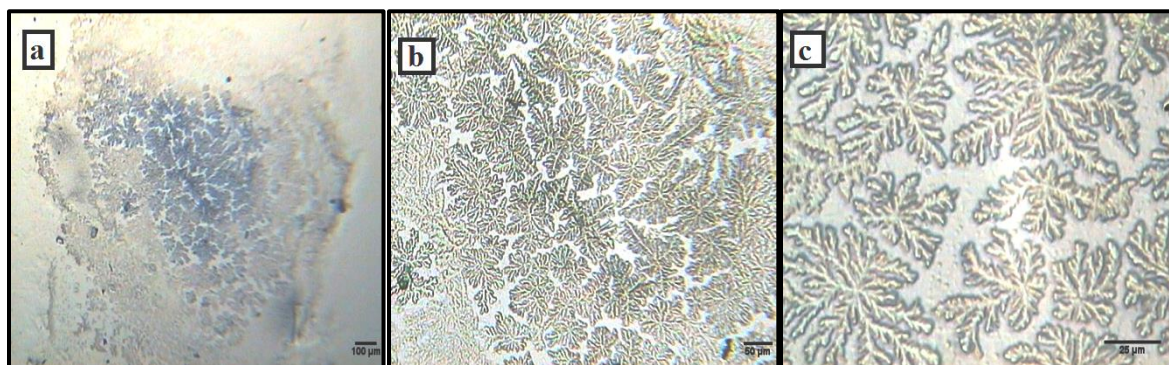


Figure 3.2 $\log_{10}(\text{box size}) - \log_{10}(\text{count})$ plot for 0.1 wt.% sodium carboxymethylcellulose with 5 mM Acetic acid (a, b) and 20 mM Acetic acid (c, d) at different magnifications.

The graphs typically depict that increasing the box size, count data rapidly decline. This demonstration reveals the fact that there is hierarchy of space sizes with few large and many small spaces, as a result there is a linear relationship between $\log_{10}(\text{box size})$ vs. $\log_{10}(\text{count})$ with correlation coefficient of 0.9971 and 0.9972 respectively that characterize the fractal “tree” pattern.

3.3.2 Effect of Acetic acid concentration with 0.2 wt.% Sodium Carboxymethyl Cellulose

Since acetic acid is monobasic weak acid with single carboxyl group having the acid dissociation constant of 4.76 which is quantitative measure of the strength of an acid in solution. Increasing the cellulose concentration (0.2 wt.%), the tree like ramified structure with fragmentation is observed at higher magnification of the drop. The images clearly manifest the fact that the formation of structure tends to grow from the periphery of the drop occupying the central region at low concentration (5 mM) of acetic acid. At higher magnification of the drop, the Figure 3.3 (c) clearly demonstrates the fractal tree like ramified structure with unique growth in all directions. However, some of the fractal structures did not grow with unique branches. This may be due to many nucleating points of the aggregates are not likely to form the fractal pattern. The self-assembled ramified structure looks similar at low and high acetic acid concentration. Only the basic difference between them is that at low concentration, the structure tends to grow with unique and less branches while at higher concentration, the structure tends to grow somewhat random and unique branches. The whole mechanism of the fractal structure manifest the diffusion limited aggregation (DLA) process but the growth is far from the equilibrium.



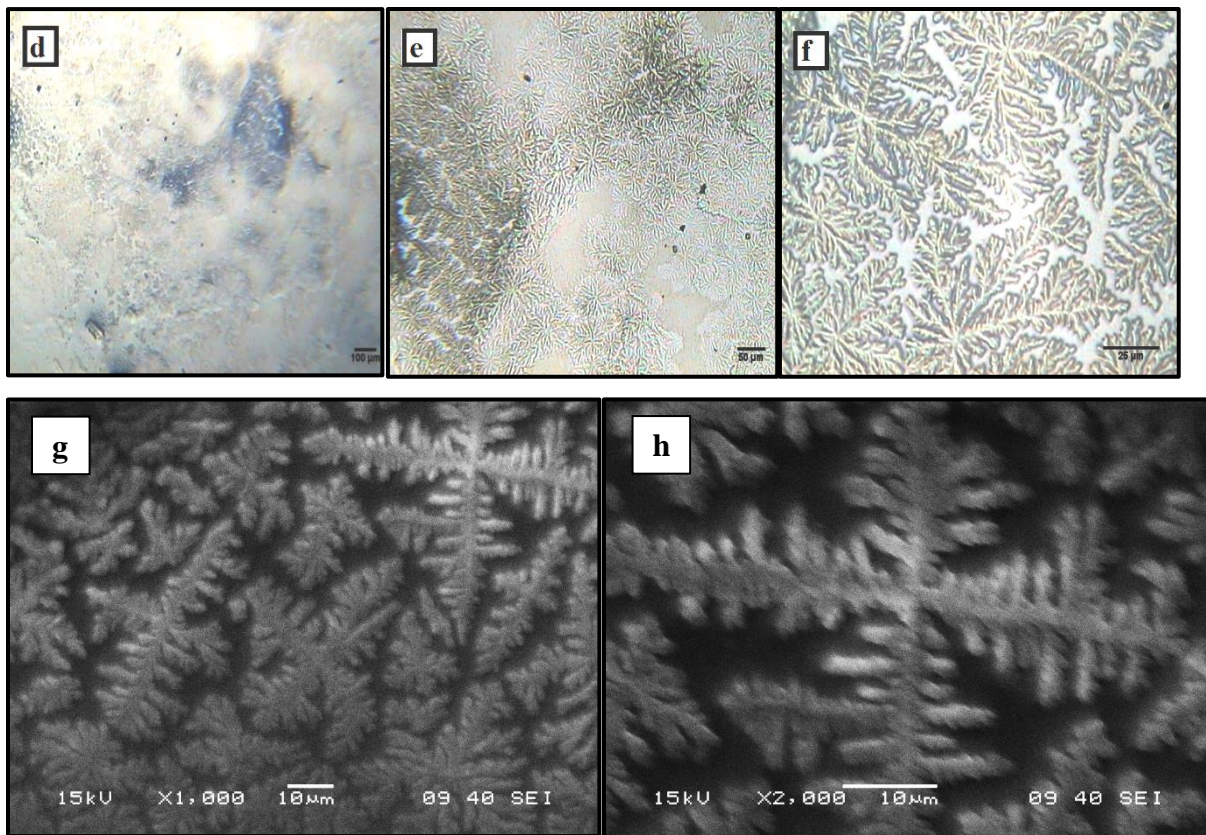


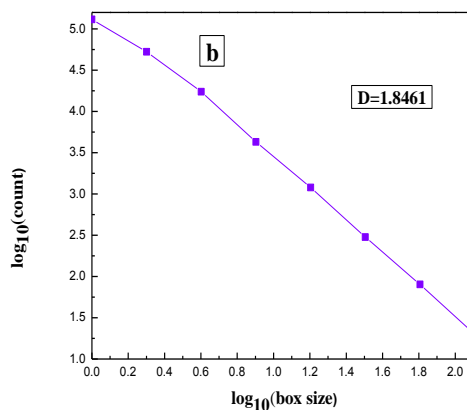
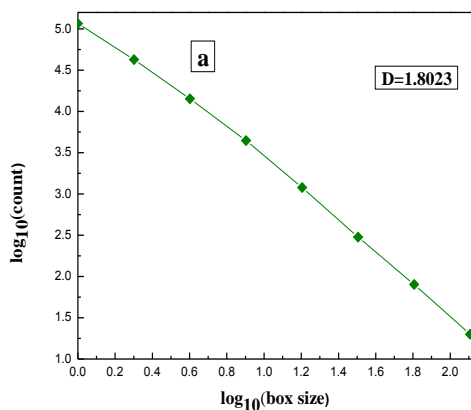
Figure 3.3 Self-assembled structure of Sodium Carboxymethyl Cellulose with 0.2 wt.% in the presence of 5 mM Acetic acid (a, b, c), SEM images (g, h) and 20 mM Acetic acid (d, e, f).

All the above patterns are recognized by fractal dimension for analyzing the images using Fractal Analysis Software (Sasaki et al., 1994). The fractal pattern at 5 mM acid concentration with 0.2 wt.% cellulose shows the fractal dimension value 1.7782 as well as less coverage percentage 33.5% at higher magnification. On the other hand, increasing the acid concentration the fractal dimension reaches to 1.8134 which is slightly higher. The structure becomes more roughness at higher fractal dimension as compared to low fractal dimension. However, these analysis show that the fractal tree like ramified structure tends to grow via diffusion limited aggregation (DLA) process with less or more effect.

Table 3.2: Fractal Analysis of images of 0.2 wt.% sodium carboxymethylcellulose with 5 mM Acetic acid (a, b, c) and 20 mM Acetic acid (d, e, f)

Image no.	Width, height	Coverage (%)	Correlation coefficient	No. of data to calculate	Fractal Dimension
a	640, 480	37.7	0.9985	8	1.8023
b	640, 480	42.3	0.9983	8	1.8461
c	640, 480	33.5	0.9978	8	1.7782
d	640, 480	37.9	0.9985	8	1.8031
e	640, 480	37.4	0.9980	8	1.8165
f	640, 480	39.2	0.9984	8	1.8134

All the structures are characterized by the graph between $\log_{10}(\text{box size})$ vs. $\log_{10}(\text{count})$ using box counting method. The slope of the graph gives the fractal dimension value. The graphs of Figure 3.4 (a, b, c) manifest 0.2 wt.% cellulose with 5 mM acid concentration at different magnifications. However, cellulose self-assembly at 20 mM acid concentration shown at Figure 3.4 (d, e, f). The plots clearly reveal the fact that count data rapidly declines with increasing the box size which are displayed on the logarithmic scale. There is continuous linear falling of count data with box size; as a result the patterns follow the fractal structures due to linearity with correlation coefficient of about 0.99.



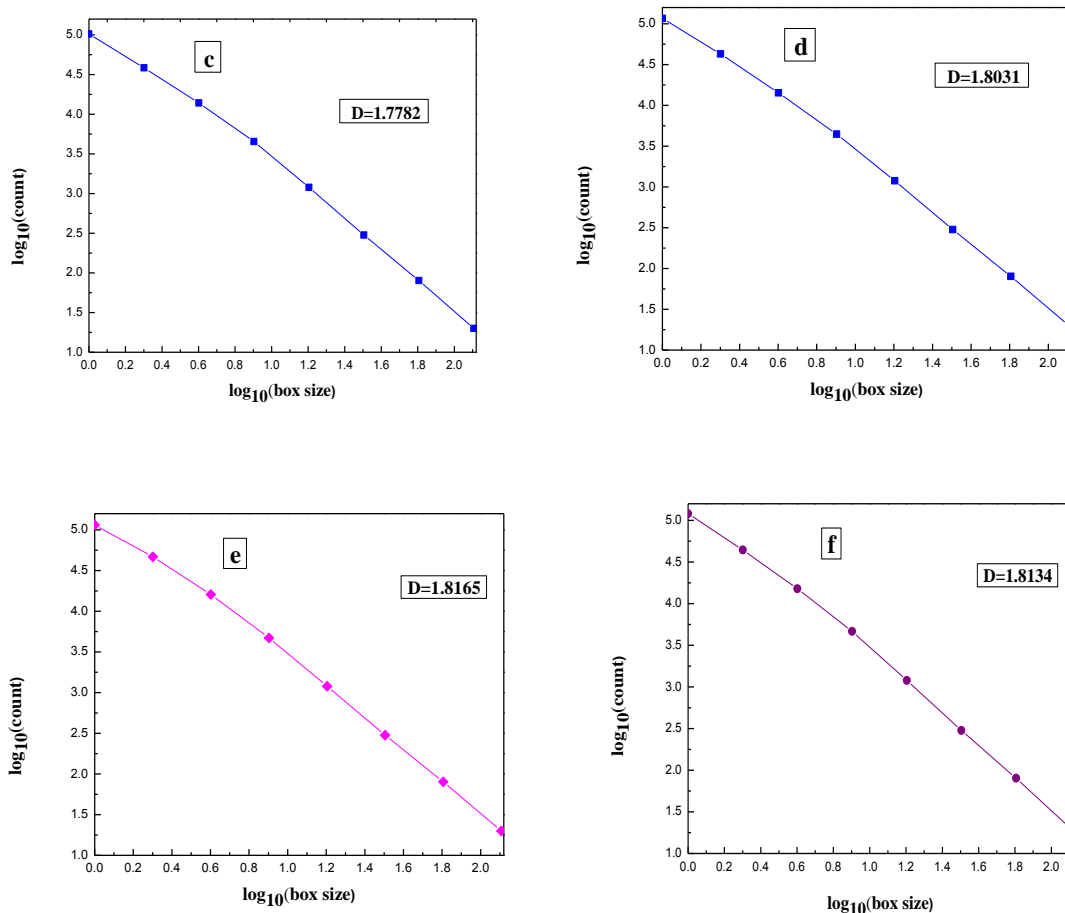


Figure 3.4 $\log_{10}(\text{box size}) - \log_{10}(\text{count})$ plot for 0.2 wt.% sodium carboxymethyl cellulose with 5 mM Acetic acid (a, b, c) and 20 mM Acetic acid (d, e, f) at different magnifications.

3.3.3 Effect of pH in the self-assembled structure of Sodium Carboxymethyl Cellulose in the presence of Acetic Acid

Fractal character of the pattern gradually increases with increasing pH, when pH increased from 3.5 to 5.3. This is due to the COONa groups on sodium carboxymethyl cellulose become deprotonated with increasing pH. As a result, the energy barrier between two neighboring branches increases and screening effect becomes strong. Screening effect arises due to the fact that the inner electron are more attracted towards the nucleus so that the inner electron will not allow the nuclear charge to pass through as a result the outer electron will get a lower nuclear charge than the inner electron. Consequently fractal trees were not obtained at lower pH values. At low pH value, cellulose molecules adhered to each other and structure becomes dense in the

formation of fractal tree like pattern. Besides the protonation effect, sodium oxalate salt also plays a crucial role in the formation of structure. Fractal dimension is another parameter to clarify the structure. It is observed from the fractal analysis that higher fractal “tree” like ramified structure with equilibrium conditions are accompanied with low fractal dimension value at higher pH. The item of coverage also changes the difference of brightness for different images as shown in Figure 3.5.

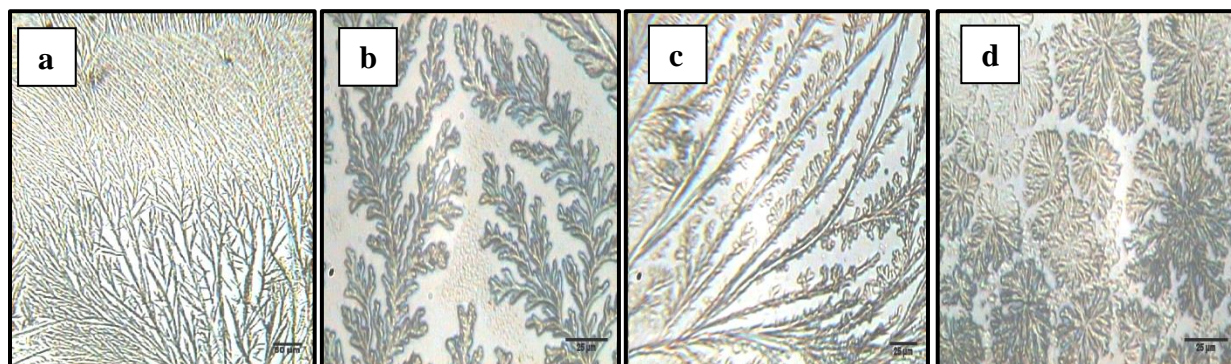


Figure 3.5 Effect of pH in the self-assembled structure of Sodium Carboxymethylcellulose (a) pH=3.5, (b) pH=4.0, (c) pH=4.5, (d) pH=5.3.

3.4 Conclusions

The structure is formed during the evaporation of liquid drop on solid surface because of crystallization of respective salt, the interplay of evaporative liquid flux and Marangoni flow inside the drop, capillary and van der Waals attractive forces. The fragmented fractal “tree” like pattern of sodium carboxymethyl cellulose is observed with oxalic acid. Some parameters are very important such as sodium carboxymethyl cellulose concentration, acid concentration, drying time, drying temperature, humidity, stirring velocity, stirring temperature, pH and drop volume for the formation of self-assembled structure. The fine structure is generated at low acid concentration while the sodium carboxymethyl cellulose concentration depends on the type of organic acid (monobasic, dibasic or tribasic). Drop volume is also an important parameter and it is observed that low drop volume lacks the pattern formation. Fractal characters of the pattern gradually disappear with decreasing pH. Fractal dimensions of these fractal patterns are in the range of 1.77 – 1.85 which follow the diffusion limited aggregation (DLA) mechanism. The box size vs. count plots on the logarithmic scale provides the linearity; as a result follow the fractal pattern.

Effect of Inorganic acid in the self-assembled structure of Sodium Carboxymethyl Cellulose

4.1 Introduction

The introductory part is same as in case of organic acid for the self-assembled structure formation of sodium carboxymethyl cellulose. Monobasic hydrochloric acid is used for the formation of self-assembled fractal pattern of sodium carboxymethyl cellulose. We have demonstrated the effect of cellulose concentration and acid concentration as well as the effect of drop volume in the formation of structure.

4.2 Materials and Method

The chemicals used in this experiment were procured from the following companies, Sodium Carboxymethyl Cellulose $[C_6H_7O_2(OH)_x(OCH_2COONa)_y]_n$ 99% purity from Loba chemicals (India), Hydrochloric acid (HCl) 35% purity from Merck (India). All chemicals were used as received without any further purification. Ultrapure water having resistivity of 18 M Ω cm and pH 6.4–6.5 was used for all the experiments.

Sodium Carboxymethyl Cellulose in aqueous media was prepared from the stock solution of higher concentration with acid. The proper mixing of cellulose and acid proceed by magnetic stirrer with continuous stirring at 600 rpm maintaining the temperature at 30°C about 20 minutes. The glass slides were initially washed with alcohol and then deionized water, and dried in a hot air oven. Then the solution was dropped onto the glass slide using a microliter syringe (Hamilton) with different drop volumes (1 μ l to 10 μ l) to study the drop volume also. Then the slides containing droplets were dried in a hot air oven at 30°C for more than 210 minutes with a constant relative humidity of 30%. The resulting dried drops were observed under an optical microscope (Hund, D600).

4.3 Results and Discussion

4.3.1 Effect of Hydrochloric acid concentration with 0.1 wt.% Sodium Carboxymethyl Cellulose

According to the basicity of acids, hydrochloric acid is monobasic strong acid having the acid dissociation constant (pKa) of -7. It means that hydrogen ions completely ionize in the solution. The exact pKa of an acid is a function of molecular structure. Here, we have demonstrated the variation in concentration of Hydrochloric acid with constant sodium carboxymethyl cellulose (0.1 wt.%). Firstly, we have observed the fractal pattern of sodium carboxymethyl cellulose with

5 mM Hydrochloric acid. It is clear from the figure 4.1 (a) that at low magnification, it follows the coffee-ring effect with growing of branches from central nucleus which shows the clear image at higher magnification and magnified image of particular branch reveals the fact that the branches grew at 90° to each other figure 4.1 (c). The formation of tree like ramified structure may be due to sodium chloride (NaCl) salt. It should be noted that formation of structure is a complex interplay of differential evaporative flux and Marangoni effect. The Marangoni effect gives way to Mullins-Sekerka instability which causes stems of the structure grow along the perimeter, towards the center from the high end of concentration gradient of the drop. The flow due to evaporative flux tends to carry the salt and particles in opposite direction, towards the perimeter of the drop. Additionally it is believed that the competition between two flows induce the sideways branching along the high energy edges of crystals in previously formed stems, instead of aiding more stem growth.

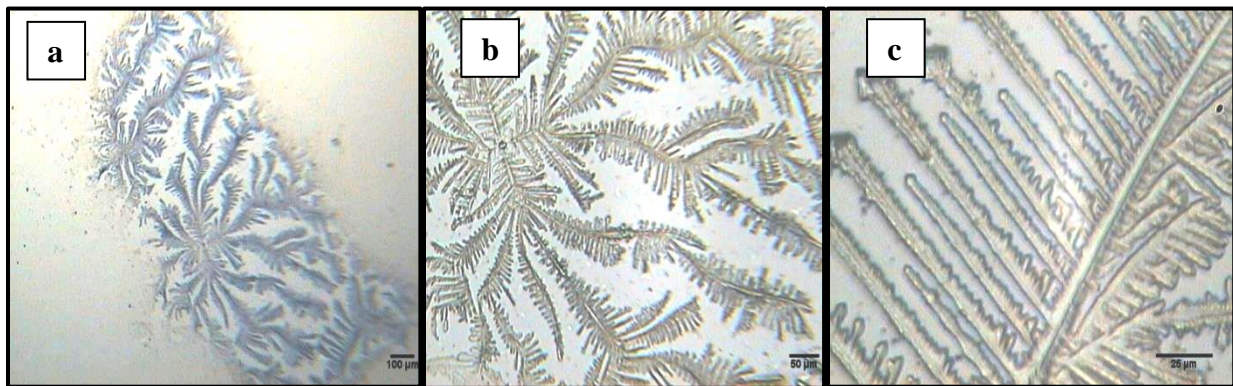
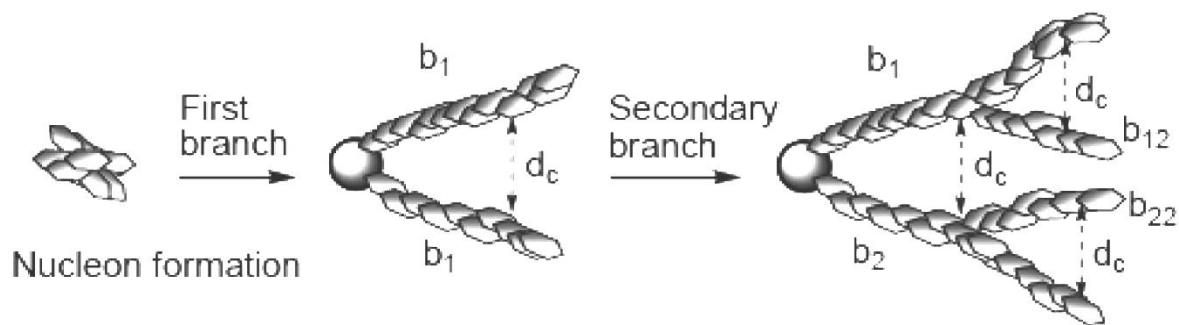


Figure 4.1 Self-assembled structure of Sodium Carboxymethyl Cellulose with 0.1 wt.% in the presence of 5 mM Hydrochloric acid at different magnifications.

The mechanism of self-assembled fractal pattern formation is as follows:



Cellulose molecules preferentially adhere to the initial nucleon via ‘random walk’ process, which causes the first generation of branches (b_1) to grow up from the nucleon. The strength of energy barrier decreases with increasing distance (d) between two neighboring branches. Consequently, a critical distance (d_c) exists, above which cellulose molecules can break the energy barrier. In other words, secondary generation of the branches (b_{12}) will automatically grow from the mother branch (b_1) when $d > d_c$. The same principle is applicable for the next generation of branches.

All the fractal patterns are analyzed by Fractal Analysis Software (Sasaki et al., 1994). In general, a set is called fractal for which the Hausdorff dimension is greater than its topological dimension. Fractal dimension reveals the quantitative measurement of smoothness or roughness of the structure. The closer fractal dimension is to one, smoother the fractal curve. Here, it is clear from the table 4.1 that there is a linear relationship between coverage percentage and fractal dimension. The magnified image of particular branch (Figure 4.1c) manifests the lower fractal dimension value corresponds to 1.7916 among all of the magnifications due to more smoothness.

Table 4.1: Fractal Analysis of images of 0.1 wt.% sodium carboxymethylcellulose with 5 mM Hydrochloric acid

Image no.	Width, height	Coverage (%)	Correlation coefficient	No. of data to calculate	Fractal Dimension
a	640, 480	37.0	0.9983	8	1.8021
b	640, 480	38.0	0.9980	8	1.8178
c	640, 480	36.8	0.9984	8	1.7916

It is observed from the figure 4.2 that increasing the acid concentration from 5 mM to 10 mM with constant (0.1 wt.%) sodium carboxymethyl cellulose concentration, the structure predominates the fragmentation step after proceeding the unstable growth and coarsening (thickening of fractal pattern formation) in the diffusion limited aggregation (DLA) growth process. The ramified fragmented structure tends to grow from the central nucleon with various branches growing in all the directions.

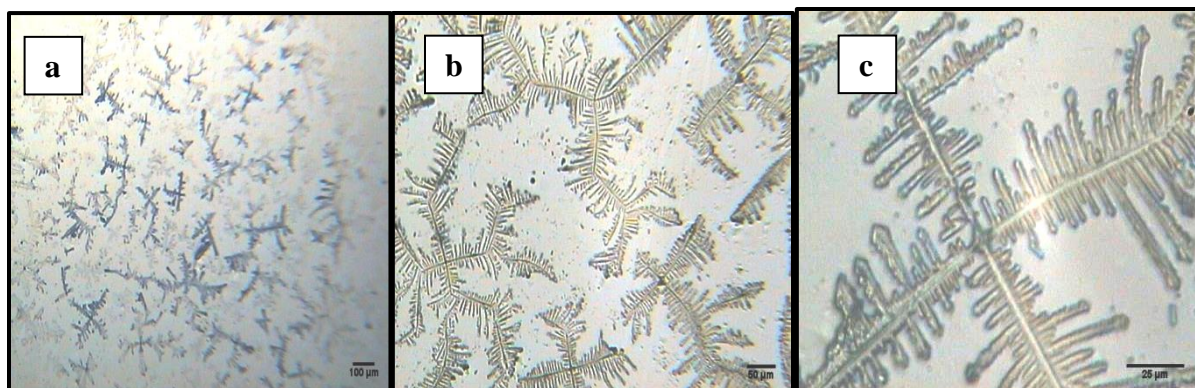


Figure 4.2 Self-assembled structure of Sodium Carboxymethyl Cellulose with 0.1 wt.% in the presence of 10 mM Hydrochloric acid at different magnifications.

All the patterns are analyzed by Fractal dimension to clarify the structure. Table 4.2 (c) reveals less fractal dimension value corresponds to 1.7755 among all of these structures. The lower fractal dimension value demonstrates the smoothness of the structure. However, all calculated fractal dimension values at different magnifications ranging from 1.7755 to 1.8255 manifests the fractal “tree” like ramified structure due to diffusion limited aggregation (DLA) growth process.

Table 4.2: Fractal Analysis of images of 0.1 wt.% sodium carboxymethylcellulose with 10 mM Hydrochloric acid

Image no.	Width, height	Coverage (%)	Correlation coefficient	No. of data to calculate	Fractal Dimension
a	640, 480	41.6	0.9988	8	1.8225
b	640, 480	34.3	0.9977	8	1.7925
c	640, 480	36.6	0.9983	8	1.7755

Now further increment of Hydrochloric acid concentration upto 20 mM with constant (0.1 wt.%) sodium carboxymethyl cellulose concentration, the tree like ramified fragmented structure tends to grow from the periphery of the drop towards the center following the coffee-ring effect at low magnification (Figure 4.3a). At higher magnification, the structure follows the same trend as before which is growing up from the central nucleus with less or more branches. The magnified image of the particular branch clearly manifests the almost unique growth in both the directions following the diffusion limited aggregation (DLA) mechanism.

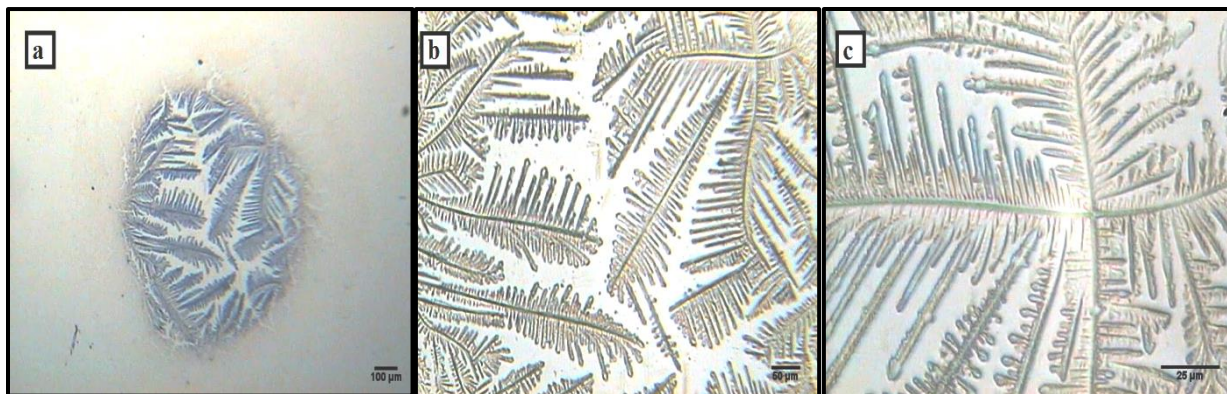
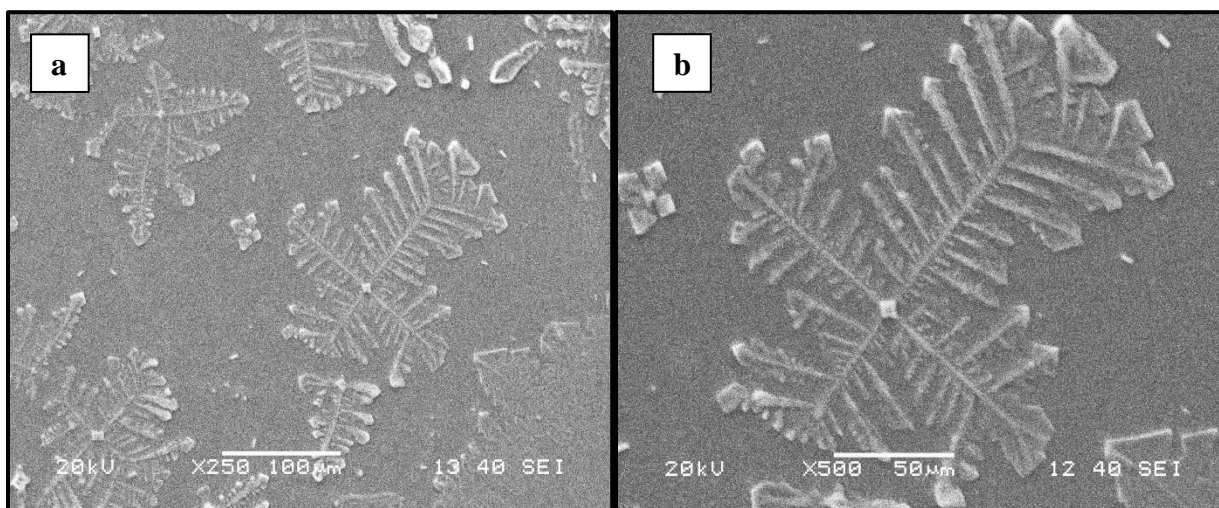


Figure 4.3 Self-assembled structure of Sodium Carboxymethyl Cellulose with 0.1 wt.% in the presence of 20 mM Hydrochloric acid at different magnifications.

Table 4.3: Fractal Analysis of images of 0.1 wt.% sodium carboxymethylcellulose with 20 mM Hydrochloric acid

Image no.	Width, height	Coverage (%)	Correlation coefficient	No. of data to calculate	Fractal Dimension
a	640, 480	38.8	0.9987	8	1.8057
b	640, 480	35.6	0.9979	8	1.7974
c	640, 480	36.2	0.9983	8	1.7926



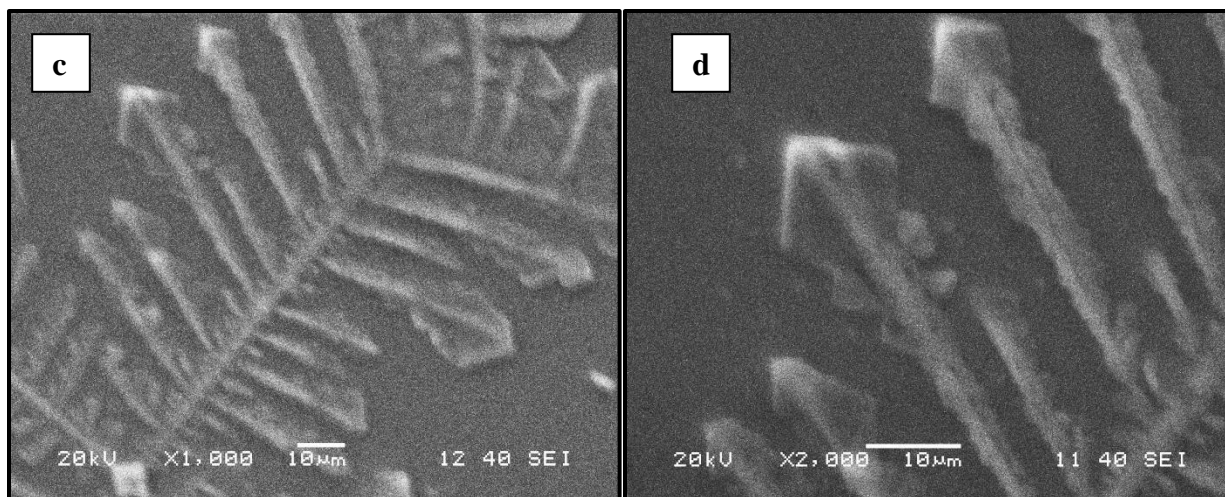


Figure 4.4 SEM images of Self-assembled structure of Sodium Carboxymethyl Cellulose with 0.1 wt.% in the presence of 20 mM Hydrochloric acid at different magnifications.

It is highly observed that “tree” like structure of sodium carboxymethyl cellulose is attained with 30 mM Hydrochloric acid. Figure 4.5 (a) clearly manifests the structure growing from periphery of the drop towards the center in the fashion of tree like with numerous branches following the “coffee-ring” effect. The structure tends to grow from the initial nucleus with distributing numerous branches in all the directions and further development of secondary branches from the mother branch. However, some branches tend to grow very rapidly as compared to others. This may be attributed to the fact that many of the nucleating points already stabilized and no further development of growth but it is also possible that some nucleating points are not well established and further branching is occur as shown in Figure 4.5 (b).



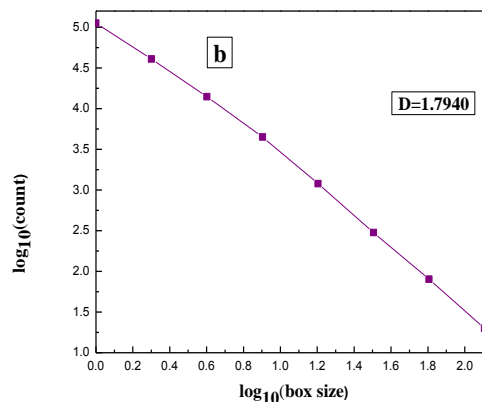
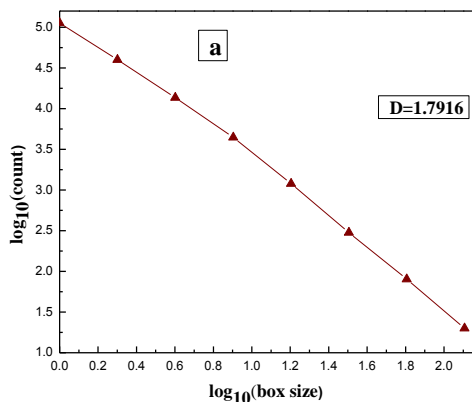
Figure 4.5 Self-assembled structure of Sodium Carboxymethyl Cellulose with 0.1 wt.% in the presence of 30 mM Hydrochloric acid at different magnifications.

Now, at higher magnification (Figure 4.5 c) the structure clearly reveals the tree like structure with some less or more growth of the branches. The structures follow the diffusion limited aggregation (DLA) mechanism which follows the four steps: unstable growth, coarsening, fragmentation and equilibrium. The growth of the structures is far away from fragmentation and equilibrium stages.

Table 4.4: Fractal Analysis of images of 0.1 wt.% sodium carboxymethylcellulose with 30 mM Hydrochloric acid

Image no.	Width, height	Coverage (%)	Correlation coefficient	No. of data to calculate	Fractal Dimension
a	640, 480	38.4	0.9983	8	1.8098
b	640, 480	36.2	0.9980	8	1.8059
c	640, 480	35.3	0.9981	8	1.7886

The graph between $\log_{10}(\text{box size}) - \log_{10}(\text{count})$ are also displayed whether to check the image is fractal or not by linearity with Fractal Analysis Software (Sasaki et al., 1994). The box-counting method provides the grids with a varying number of boxes are superimposed on an image of the pattern of interest. Fractal pattern introduces spaces of a range of sizes. So that there is hierarchy of space sizes including few large and many small spaces. The inset of box counting is to quantify fractal scaling but from a practical perspective this would require the scaling be known. The graphs (Figure 4.6) clearly manifest the fractal structure of sodium carboxymethylcellulose at different concentrations of Hydrochloric acid.



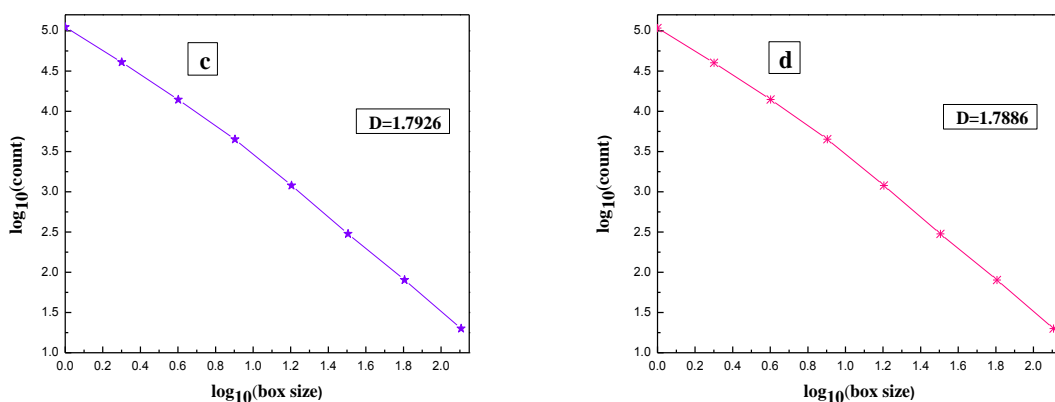


Figure 4.6 $\log_{10}(\text{box size}) - \log_{10}(\text{count})$ plot for 0.1 wt.% sodium carboxymethylcellulose with (a) 5 mM Hydrochloric acid (b) 10 mM Hydrochloric acid (c) 20 mM Hydrochloric acid (d) 30 mM Hydrochloric acid at 400X magnification.

4.3.2 Effect of Hydrochloric acid concentration with 0.01 wt.% Sodium Carboxymethyl Cellulose

The self-assembled sodium carboxymethyl cellulose structures are also observed at 0.01 wt.% with the variation in Hydrochloric acid concentration. Firstly, the self-assembled structures are observed with 5 mM Hydrochloric acid concentration and it is found that pattern tends to grow in dendritic form and eventually attained the dense branching morphology structure (Figure 4.7 a). However, at higher magnification the structure clearly reveals the fact that branches grow from the main stem with 90° to each other containing the same lacunarity (Figure 4.7 b). It has seen from the Figure 4.7 (c, d) that increasing the acid concentration upto 10 mM, the structure tends to grow from the main stem with numerous branches following the diffusion limited aggregation (DLA) mechanism in which the crystal growth and coarsening stages are predominant as compared to fragmentation and equilibrium conditions. Now, further increment of acid concentration upto 20 mM, the fragmented structure tends to grow in unique directions after preceding the unstable growth and coarsening steps (Figure 4.7 e).

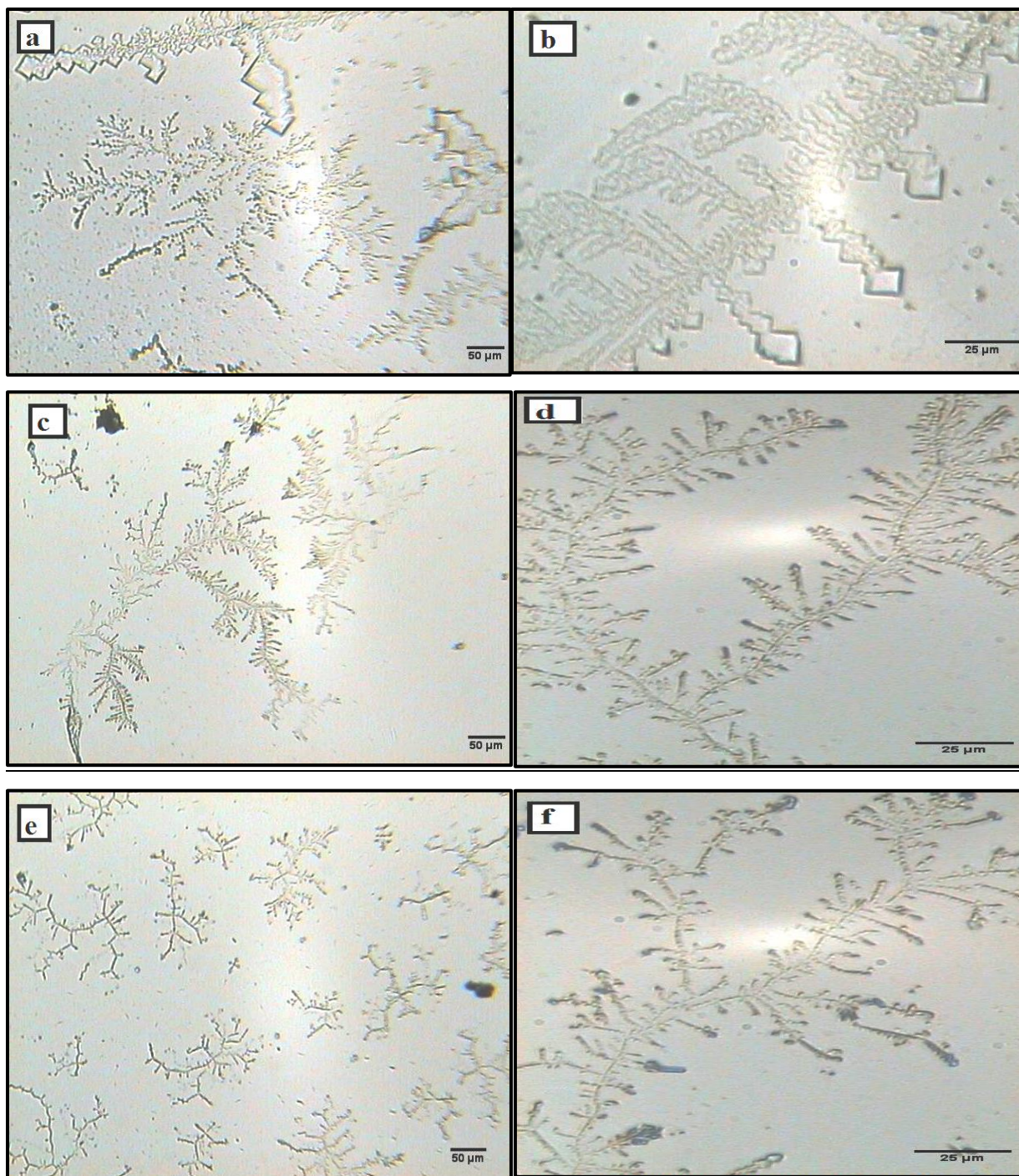


Figure 4.7 Self-assembled structures of sodium carboxymethyl cellulose (0.01 wt.%) with 5 mM Hydrochloric acid (a, b), 10 mM Hydrochloric acid (c, d), and 20 mM Hydrochloric acid (e, f); scale bars indicate 50 microns (a, c, e) and 25 microns (b, d, f).

All the structures are analyzed by fractal dimension using Fractal Analysis Software (Sasaki et al. 1994). Actually, measuring the fractal dimension does not necessarily mean determining if something has a fractal form. It basically measures the smoothness or roughness of pattern. Calculated fractal dimension values manifest the diffusion limited aggregation (DLA) mechanism ranging from 1.7381 to 1.8076. The highest value of fractal dimension corresponds to more roughness which is attained at 20 mM acid concentration. However, coverage percentage also affects the fractal dimension. The table 4.5 clearly depicts the fact that fractal dimension continuously increases with increasing the coverage percentage (which determines the difference of brightness of the image).

Table 4.5: Fractal Analysis of images of 0.01 wt.% sodium carboxymethylcellulose with 5 mM Hydrochloric acid (a, b), 10 mM Hydrochloric acid (c, d) and 20 mM Hydrochloric acid (e, f)

Image no.	Width, height	Coverage (%)	Correlation coefficient	No. of data to calculate	Fractal Dimension
a	640, 480	31.3	0.9974	8	1.7721
b	640, 480	29.9	0.9973	8	1.7615
c	640, 480	26.3	0.9965	8	1.7381
d	640, 480	28.9	0.9971	8	1.7547
e	640, 480	30.6	0.9972	8	1.7698
f	640, 480	37.6	0.9983	8	1.8076

Another important parameter to characterize the images is box-counting method. Generally, it is assumed to assign the smallest number of boxes to cover the entire image. Box size refers to the size of individual boxes in one grid of a series of grids which is used to measure an object and count usually refers the number of grid boxes that contained pixels in box-counting scan. The plots clearly analyze the structures whether it is fractal or not by linearity. Here, in all the cases it is found that eight boxes are calculated and as increases the box size, count rapidly declines. It means numbers of grid boxes are less with higher box size.

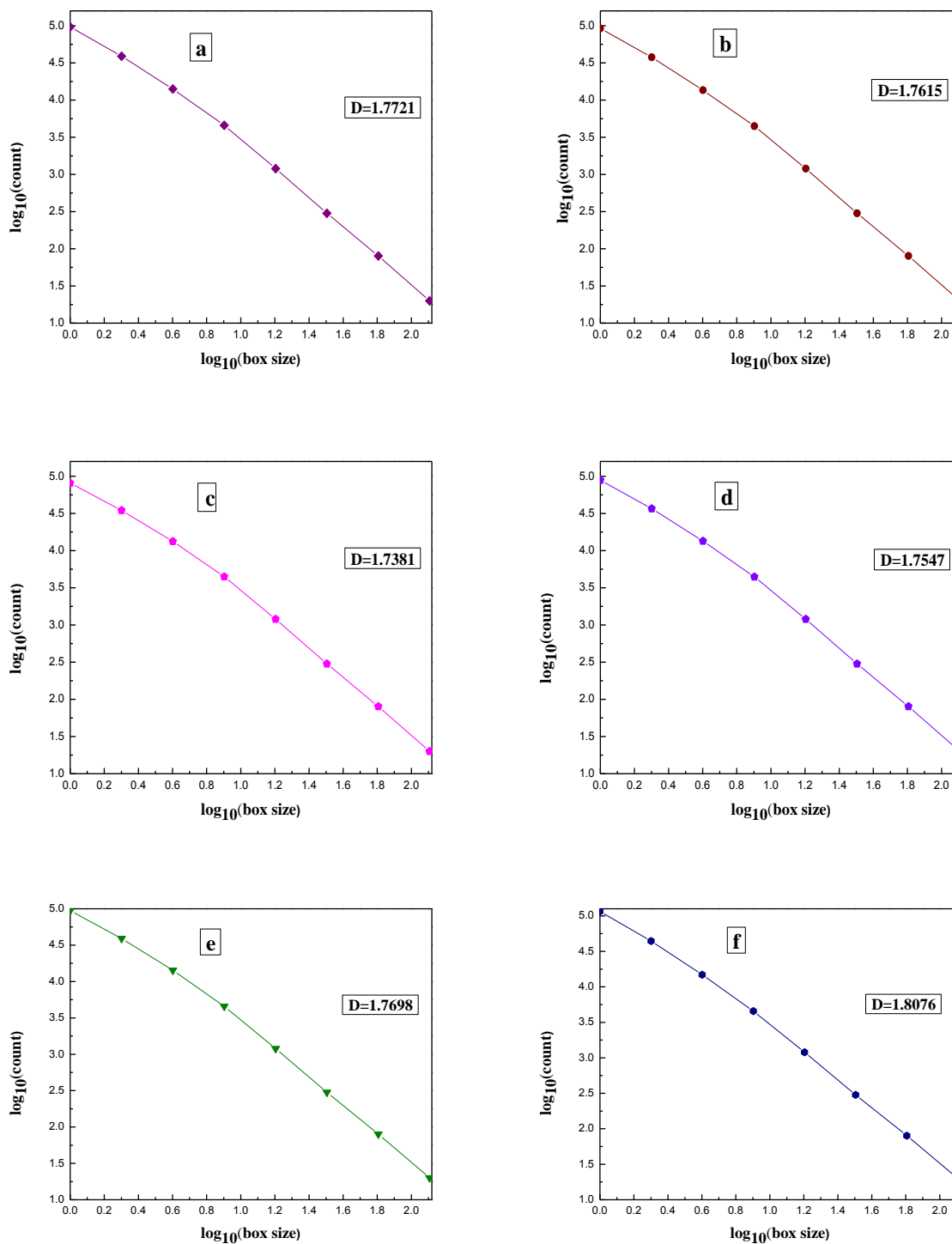
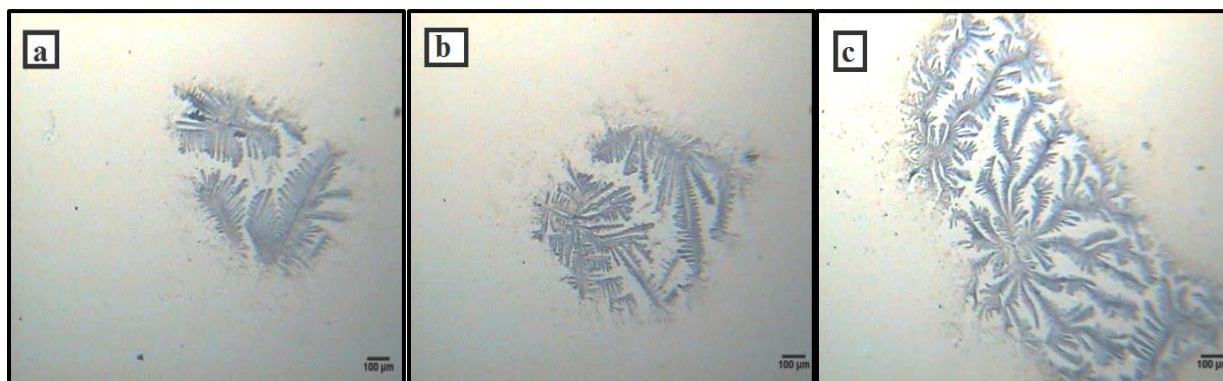


Figure 4.8 $\log_{10}(\text{box size}) - \log_{10}(\text{count})$ plot for 0.01 wt.% sodium carboxymethylcellulose with (a, b) 5 mM Hydrochloric acid, (c, d) 10 mM Hydrochloric acid, and (e, f) 20 mM Hydrochloric acid at different magnifications.

4.3.3 Effect of drop volume in the self-assembled structure of 0.1 wt.% Sodium Carboxymethyl Cellulose with 5 mM Hydrochloric acid

Drop volume is an important parameter playing a major role in the formation of structure. Here, we have demonstrated 0.1 wt.% sodium carboxymethyl cellulose with low concentration of hydrochloric acid. Higher concentrations were not chosen so as to avoid the disjoining pressure effect (Kondiparty et al., 2011) due to presence of higher number of particles, which will cause the drop to spread out more and increase in surface area causing quick drying. Gradual changes (proper growth of branches, elongation in the main stem length) in the structure are clearly visible with increase in drop volume as depicted in Figure 4.9. When the drop volume increases the drop area on the solid surface as well as the drop height also increases. In general, during the evaporation of drop from the solid surface, the presence of particles causes the drop boundary to be fixed to its initial position till a certain time. However, when drop size is small, the drop height is also less; as a result the evaporation of drop is fast. For small drops, the evaporative flux is not large enough to transport the particles to periphery of the drop. The larger drop volume (10 μ l) clearly manifests the structure (Figure 4.9 c, f) growing from the periphery of the drop towards the central region due to particles have sufficient time to reach periphery and circulate back to the center to form the self-assembly. Generally, when the drop height is sufficiently higher than the average particle size present in the media, and if evaporative flux is enough to move the particles of all sizes towards the periphery and circulate them, a uniform self-assembled structure with well-developed branches and long stems was formed.



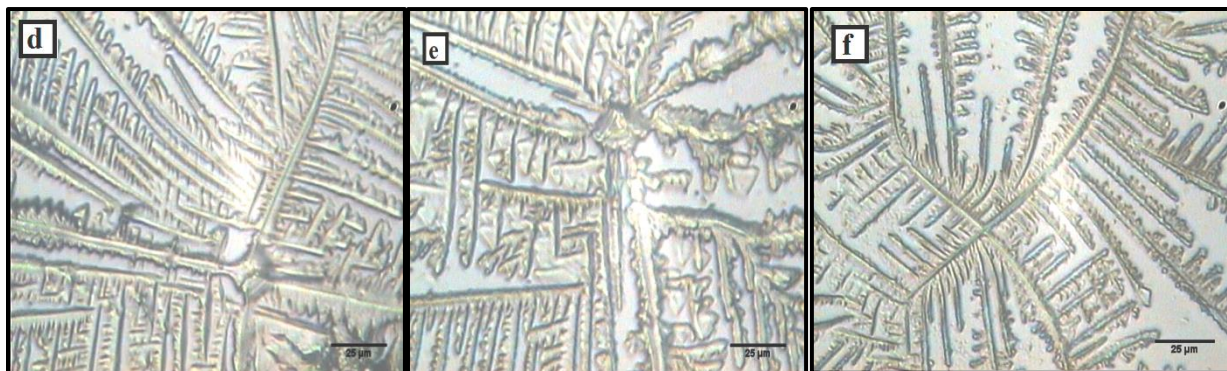


Figure 4.9 Self-assembled structures of sodium carboxymethyl cellulose with 5 mM Hydrochloric acid (a) 1 μl , (b) 5 μl and (c) 10 μl drops and their respective magnified images (d, e, f); scale bars indicate 100 microns (a, b, c) and 25 microns (d, e, f).

4.4 Conclusions

The fractal “tree” like patterns also observed in case of inorganic acids but some important parameters effect in the formation of structure as described above. It is observed that for monobasic acid (Hydrochloric acid), the structure is self-assembled at 0.1 wt.% cellulose concentration but at ten times lower concentration (0.01 wt.%) the structure follows the confinement. However, increasing the acid concentration or decreasing the cellulose concentration, the fractal structure changes. Drop volume is also an important parameter and the results demonstrate that low drop volume lacks the pattern formation.

Conclusions and Suggestions for Future work

5.1 Conclusions

The overall findings of this work can be summarized as follows:

The structure is formed during the evaporation of liquid drop on solid surface because of crystallization of respective salt, the interplay of evaporative liquid flux and Marangoni flow inside the drop, capillary and van der Waals attractive forces. The fragmented fractal “tree” like pattern of sodium carboxymethyl cellulose is observed with oxalic acid. Some parameters are very important such as sodium carboxymethyl cellulose concentration, acid concentration, drying time, drying temperature, humidity, stirring velocity, stirring temperature, pH and drop volume for the formation of self-assembled structure. The fine structure is generated at low acid concentration while the sodium carboxymethyl cellulose concentration depends on the type of organic acid (monobasic, dibasic or tribasic). Fractal characters of the pattern gradually disappear with decreasing pH. Fractal dimensions of these fractal patterns are in the range of 1.77 – 1.85 which follow the diffusion limited aggregation (DLA) mechanism. The box size vs. count plots on the logarithmic scale provides the linearity; as a result follow the fractal pattern.

In the next study, the fractal “tree” like patterns is also observed in case of inorganic acid but some important parameters effect in the formation of structure as described above. It is observed that for monobasic (hydrochloric acid), the structure is self-assembled at 0.1 wt.% cellulose concentration but at ten times lower concentration (0.01 wt.%) the structure follows the confinement. However, increasing the acid concentration or decreasing the cellulose concentration, the structure changes from fractal to self-assembled nanorods. Drop volume is also an important parameter and the results demonstrate that low drop volume lacks the pattern formation.

5.2 Suggestions for Future work

This work can be further extended and deeply explored. There is virtually no limitation to raw materials that can be used for self-assembly and fabrication of functionalized structures and new materials. In the future, the following work can be done:

- (1) Similar self-assemblies can be tried with other materials as the mobile components such as polystyrene microspheres, glass microbeads, silica, starch and so on.
- (2) Different solvents may also show variation in the structure.
- (3) More crystalline and semicrystalline materials can be explored to assist and enhance the structure forming abilities of the particles.
- (4) More detailed studies using contact angle meter as well as atomic force microscope can be done. This will help to generate drying pattern, drop stain texture and topology data.
- (5) The structure can be functionalized with other materials as per the requirement or application such as enhancement of the performance of dye sensitized solar cells using polymer electrolyte.

References

Bai, F.; Zeng, C.; Yang, S.; Zhang, Y.; He, Y.; Jin, J. “The formation of a novel supramolecular structure by amyloid of poly-L-glutamic acid”, *J. Biochem. Biophys. Res. Commun.* (2008), 369, 830–834.

Banerjee, R.; Hazra, S.; Banerjee, S.; Sanyal, M. K. “Nanopattern formation in self-assembled monolayers of thiol-capped Au nanocrystals”, *Phys.Rev. E* (2009), 80, 056204.

Brune, H.; Romainczyk, C.; Roder, H.; Kern K. “Mechanism of the transition from fractal to dendritic growth of surface aggregates”, *Nature* (1994), 369, 9, 469-471.

Cai, Y.; Newby, Bi-min Z. “Marangoni Flow-Induced Self-Assembly of Hexagonal and Stripelike Nanoparticle Patterns”, *J. Am. Chem. Soc.* (2008) 130, 6076–6077.

Chiu, C.-Wei; Lee, T.-Chien; Hong, P.-Da; Lin, J.-Jen “Controlled self-assemblies of clay silicate platelets by organic salt modifier” *J. Royal Society of Chemistry* (2012), 2, 8410–8415.

Chon, C. H.; Paik, S.; Jr., J. B. T.; Kihm, K. D. “Effect of Nanoparticle Sizes and Number Densities on the Evaporation and Dryout Characteristics for Strongly Pinned Nanofluid Droplets”, *Langmuir* (2007), 23, 2953-2960.

Conti, M.; Meerson, B.; Sasorov, P. V. “Breakdown of Scale Invariance in the Phase Ordering of Fractal Clusters”, *Phys. Rev. Letters* (1998), 80, 21, 4693-4696.

Dai, L. L.; Sharma, R.; Wu C. Y. “Self-Assembled Structure of Nanoparticles at a Liquid-Liquid Interface”, *Langmuir* (2005), 21, 2641-2643.

Deegan, R. D.; Bakajin, O.; Dupont, T. F.; Huber, G.; Nagel, S. R.; Witten, T. A. “Capillary flow as the cause of ring stains from dried liquid drops”, *Nature* (1997), 389, 827-829.

Denkov, N. D.; Veleev, O. D.; Kralchevsky, P. A.; Ivanov, I. B.; Yoshimura, H.; Nagayama, K. “Mechanism of Formation of Two-Dimensional Crystals from Latex Particles on Substrates”, *Langmuir* (1992), 8, 3183-3190.

Girard, F.; Antoni, M.; Sefiane, K. “On the Effect of Marangoni Flow on Evaporation Rates of Heated Water Drops”, *Langmuir* (2008), 24, 17, 9207-9210.

Gunn, E.; Wong, L.; Branham, C. W.; Marquardt B.; Kahr, B. “Extinction mapping of polycrystalline patterns”, *CrystEngComm*(2011), 13, 1123–1126.

Holtz, J. H; Asher S. A. “Polymerized colloidal crystal hydrogel films as intelligent chemical sensing materials”, *Nature* (1997), 389, 829-832.

Jason, N. N.; Chaudhuri, R. G.; Paria, S. “Self-assembly of colloidal sulfur particles influenced by sodium oxalate salt on glass surface from evaporating drops”, *Soft Matter* (2012), 8, 3771-3780.

Kaya, D.; Belyi, V. A.; Muthukumara, M. “Pattern formation in drying droplets of polyelectrolyte and salt”, *J. Chem. Phys.* (2010),133, 114905-1-8.

Kralchevskyt, P. A.; Nagayama, K. “Capillary Forces between Colloidal Particles”, *Langmuir* (1994), 10, 23-36 23.

Kundu, S.; Wang, K.; Liang, H. “Size-Controlled Synthesis and Self-Assembly of Silver Nanoparticles within a Minute Using Microwave Irradiation”, *J. Phys. Chem. C* (2009), 113, 134–141.

Lee, I.; Ahn, J. S.; Hendricks, T. R. “Patterned and Controlled Polyelectrolyte Fractal Growth and Aggregations”, *Langmuir* (2004), 20, 2478-2483.

Li, J.; Du, Q.; Sun, C. “An improved box-counting method for image fractal dimension estimation”, *Pattern Recognition* (2009), 42, 2460 – 2469.

Mullins, W. W.; Sekerka, R. F. “Morphological Stability of a Particle Growing by Diffusion or Heat Flow”, *J.Appl. Phys.* (1963), 34, 323-329.

Nagayama, K. “Two-dimensional self-assembly of colloids in thin liquid films”, *Colloids and Surfaces A* (1996), 109, 363-374.

Nakashima, H.; Furukawa, K.; Kashimura, Y.; Torimitsu. K. “Self-Assembly of Gold Nanorods Induced by Intermolecular Interactions of Surface-Anchored Lipids”,*Langmuir*(2008), 24, 5654-5658.

Nellimoottil, T. T.; Rao, P.N.; Ghosh, S. S.; Chattopadhyay A. “Evaporation-Induced Patterns from Droplets Containing Motile and Nonmotile Bacteria”, *Langmuir* (2007), 23, 8655-8658.

Newkome, G. R.; Shreiner, C. D. “Poly(amidoamine), polypropylenimine, and related dendrimers and dendrons possessing different 1-2 branching motifs: An overview of the divergent procedures”, *Polymer* (2008), 49, 1-173.

Nie, Z.; Petukhova, A.; Kumacheva, E. “Properties and emerging applications of self-assembled structures made from inorganic nanoparticles”, *Nature* (2010), 5, 15-25.

Olgun U.; Sevinc. V. “Evaporation induced self-assembly of zeolite A micropatterns due to the stick–slip dynamics of contact line”, *Powder Technology* (2008), 183, 207–212.

Park, J.; Moon, J. “Control of Colloidal Particle Deposit Patterns within Picoliter Droplets Ejected by Ink-Jet Printing”, *Langmuir* (2006), 22, 3506-3513.

Paunov, V. N.; Kralchevsky, P. A.; Denkov, N. D.; Nagakama, K. “Lateral Capillary Forces Between Submillimeter Particles”, *Colloid and Interfacial Science* (1993), 57, 100-112.

Prasada R. R.; Sreenivasan, K. R.” The measurement and interpretation of fractal dimensions of the scalar interface in turbulent flows” *J. Phys. Fluids A* (1990), 2, 5, 792-807.

Sasaki, H.; Shibata, S.; Hatanaka T. “An Evaluation Method of Ecotypes of Japanese Lawn Grass for Three Different Ecological Functions”, *Natl. Grassl. Res. Inst.* 49: 17-24.

Sharon, E.; Moore, M. G.; McCormick, W. D.; Swinney, H. L. “Coarsening of Fractal Viscous Fingering Patterns”, *Phys. Review Letters* (2003), 91, 20, 205504-1 – 205504-4.

Shenhar R.; Norsten T. B.; Rotello V. M. “Polymer-Mediated Nanoparticle Assembly: Structural Control and Applications”, *Adv. Mater.* (2005), 17, 6, 657-669.

Shukla, N.; Nigra, M. M. “Synthesis and self-assembly of magnetic nanoparticles”, *J. Surface Science* (2007), 601, 2615–2617.

Takhistov, P., Chang, H.-chiam “Complex Stain Morphologies”, *Ind. Eng. Chem. Res.* (2002), 41, 6256-6269.

Tong, X.; Zhao, Y.; Huang, T.; Liu, H.; Liew, K. Y. ”Controlled synthesis of pompon-like self-assemblies of Pd nanoparticles under microwave irradiation” *J. Appl. Surface Science* (2009), 255, 9463–9468.

Witten T. A.; Sander, L. M. “Diffusion-limited aggregation”, *Phys. Rev. B* (1983), 27, 9, 5686-5697.

Xiang, J. Y.; Tu, J. P.; Zhang, L.; Zhou, Y.; Wang, X. L.; Shi, S. J. “Self-assembled synthesis of hierarchical nanostructured CuO with various morphologies and their application as anodes for lithium ion batteries”, *J. Power Sources* (2010), 195, 313–319.

Yamaki, M.; Higo, J.; Nagayama, K. “Size-Dependent Separation of Colloidal Particles In Two-Dimensional Convective Self-Assembly”, *Langmuir* (1995), 11, 2975-2978.

Yip, Hin-L.; Hau, S. K.; Baek, N. S.; Ma, H.; Jen Alex K.-Y. “Polymer Solar Cells That Use Self-Assembled-Monolayer- Modified ZnO/Metals as Cathodes”, *Adv. Mater.*(2008), 20, 2376–2382.

Yunker, P. J.; Still, T.; Lohr, M. A.; Yodh, A. G. “Suppression of the coffee-ring effect by shape-dependent capillary interactions”, *Nature* (2011), 476, 308-311.

Zhao, Q.; Qian, J.; Gui, Z.; An, Q.; Zhu, M. “Interfacial self-assembly of cellulose-based polyelectrolyte complexes: pattern formation of fractal trees”, *Soft Matter* (2010), 6, 1129-1137.

Zhao, Q.; An, Q.; Qian, J.; Wang, X.; Zhou, Y. “Insight into Fractal Self-Assembly of Poly(diallyldimethylammonium chloride)/Sodium Carboxymethyl Cellulose Polyelectrolyte Complex Nanoparticles”, *J. Phys. Chem. B* (2011), 115, 14901–14911.

Selected for conference

- Rohit Omar and Santanu Paria. “**Effect of Electrolytes on Solubilization of Naphthalene in Cationic Micellar Solutions**”. Chemference-2012 (IIT Bombay and ICT Mumbai), December 10-11, 2012.